

PhotoBench: Beyond Visual Matching Towards Personalized Intent-Driven Photo Retrieval

Tianyi Xu*
crimsonflag@sjtu.edu.cn
Shanghai Jiao Tong University
Shanghai, China

Rong Shan*
shanrong@sjtu.edu.cn
Shanghai Jiao Tong University
Shanghai, China

Junjie Wu*
wujunjie1@oppo.com
OPPO
Shenzhen, China

Jiadeng Huang
huangjiadeng@oppo.com
OPPO
Shenzhen, China

Teng Wang
wt0318@connect.hku.hk
OPPO
Shenzhen, China

Jiachen Zhu, Wenteng Chen
{gebro13,cwt-03}@sjtu.edu.cn
Shanghai Jiao Tong University
Shanghai, China

Minxin Tu, Quantao Dou
{tuminxin,douquantao}@oppo.com
OPPO
Shenzhen, China

Zhaoxiang Wang
steven.wangzx@gmail.com
OPPO
Shenzhen, China

Changwang Zhang†
changwangzhang@foxmail.com
OPPO
Shenzhen, China

Weinan Zhang†
wnzhang@sjtu.edu.cn
Shanghai Jiao Tong University
Shanghai, China

Jun Wang†
junwang.lu@gmail.com
OPPO
Shenzhen, China

Jianghao Lin†
linjianghao@sjtu.edu.cn
Shanghai Jiao Tong University
Shanghai, China

Abstract

Personal photo albums are not merely collections of static images but *living, ecological archives* defined by temporal continuity, social entanglement, and rich metadata, which makes the personalized photo retrieval non-trivial. However, existing retrieval benchmarks rely heavily on context-isolated web snapshots, failing to capture the *multi-source reasoning* required to resolve authentic, intent-driven user queries. To bridge this gap, we introduce **PHOTOBENCH**, the first benchmark constructed from authentic, personal albums. It is designed to shift the paradigm from visual matching to personalized multi-source intent-driven reasoning. Based on a rigorous *multi-source profiling* framework, which integrates visual semantics, spatial-temporal metadata, social identity, and temporal events for each image, we synthesize complex intent-driven queries rooted in users' life trajectories. Extensive evaluation on PHOTOBENCH exposes two critical limitations: the **modality gap**, where unified embedding models collapse on non-visual constraints, and the **source fusion paradox**, where agentic systems perform poor tool orchestration. These findings indicate that the next frontier in personal multimodal retrieval lies beyond unified embeddings, necessitating robust agentic reasoning systems capable of precise constraint satisfaction and multi-source fusion. Our PHOTOBENCH is available¹.

1 Introduction

Personal photo galleries have evolved from static storage into the primary repository of human memory. Unlike curated web-scale datasets (e.g., LAION [31] or MSCOCO [19]) where images are

isolated snapshots of visual content, a personal album is a *living, ecological archive*. It is temporally continuous, socially entangled, and deeply personalized. In this context, user queries are not merely simple visual descriptions (e.g., *a black dog*), but intent-driven requests anchored in heterogeneous signals, such as specific events, social relationships, or spatial-temporal constraints (e.g., *the dinner with my parents before the flight*). Consequently, effective retrieval requires not merely visual matching, but *multi-source reasoning* to fuse visual perception with user-specific context.

Despite the rapid progress in multimodal retrieval, existing benchmarks are generally **non-personalized** and fail to capture this ecological complexity, as summarized in Table 1. We identify two critical limitations in current research:

- **Lack of Ecological Fidelity (Image Gap)**. Benchmarks like MSCOCO [19] or Flickr30k [29] focus on web-scraped, context-isolated images. They lack the *temporal continuity* and *rich metadata* (timestamps, GPS, identity graphs) inherent to personal albums, rendering them unsuitable for testing temporal- or social-based complex reasoning.
- **Shallow User Intent (Query Gap)**. Datasets such as INQUIRE [39] or VisualNews [20] often rely on descriptive captions that map directly to visual content, which is usually sparse, incomplete one-to-one mapping. They fail to capture the *multi-source entanglement* and *evolving user intent* of real-world queries, where visual signals must be fused with non-visual constraints (e.g., specific time or social role) to resolve the ambiguity.

To this end, we introduce **PHOTOBENCH**, a diagnostic benchmark explicitly designed to shift the field of multimodal retrieval from *visual matching* to *personalized intent-driven reasoning*. Unlike prior efforts, PHOTOBENCH is constructed from authentic, personal

*Equal Contribution.

†Corresponding author.

¹<https://github.com/LaVieEnRose365/PhotoBench>

Table 1: We compare PHOTOBENCH with existing vision-language or multimodal retrieval datasets, highlighting its unique characteristics for real-world personalized photo retrieval tasks. *Quality Var.*: Image Quality Variance (e.g., blur, noise); *Near-dup.*: Near-duplicate burst shots.

Dataset	Query Dimensions							Image Dimensions					
	One-to-Many	Unmatched	Narrative	Personalized	Multi-Source	Reasoning	Volume	Personalized	Metadata	Temporal	Quality Var.	Near-dup.	Candidates
MSCOCO_t2i [19]	✗	✗	✗	✗	✗	✗	500K	✗	✗	✗	✗	✗	123K
Flickr30k [29]	✗	✗	✗	✗	✗	✗	16K	✗	✗	✗	✗	✗	31K
Winoground [36]	✗	✗	✗	✗	✗	✓	800	✗	✗	✗	✗	✗	2
INQUIRE [39]	✓	✗	✗	✗	✗	✓	250	✗	✓	✓	✓	✓	5M
VisDial [7]	✗	✗	✓	✗	✓	✓	1.2M	✗	✗	✗	✗	✗	100
VisualNews [20]	✗	✗	✓	✗	✓	✓	1.1M	✗	✓	✗	✓	✓	1M
Wiki-SS-NQ [24]	✓	✓	✗	✗	✓	✓	10K	✗	✓	✗	✓	✗	1M
PhotoBench	✓	✓	✓	✓	✓	✓	1.1K+	✓	✓	✓	✓	✓	1K

albums, preserving the natural noise, burstiness, and metadata headers of real-world photography. We employ a rigorous *multi-source profiling* to model each photo not merely as pixels, but as an information union of visual semantics \mathcal{V} , spatial-temporal metadata \mathcal{M} , social identity \mathcal{F} , and temporal events \mathcal{E} . Furthermore, we conduct *intent-driven query synthesis* by conditioning query generation on the multi-source information and the user’s life trajectory. In this way, we reconstruct the latent motivation behind the visual photos. Finally, through *exhaustive ground truth mining and verification*, we produce complex queries associated with a comprehensive ground truth set, which necessitates cross-modal reasoning in heterogeneous, personalized contexts. Moreover, we also synthesize zero-ground-truth queries to evaluate a retrieval system’s rejection capability to resist the user’s “false memory”.

Evaluating on SOTA retrieval models and systems, PHOTOBENCH exposes critical architectural failures that remain hidden in standard benchmarks. Our experiments reveal two critical phenomena:

- **Modality Gap.** Unified embedding models (e.g., VLM2Vec [25]) collapse when queries require precise non-visual constraints (Metadata or Face), revealing that they function primarily as visual similarity calculators rather than holistic multi-source reasoners.
- **Source Fusion Paradox.** While agentic retrieval systems equipped with external tools outperform embedding models, they exhibit a non-linear performance degradation as query complexity increases. We find that strong single-source capabilities do not automatically translate to reliable multi-source fusion, highlighting a fundamental bottleneck in *tool orchestration* and *constraint satisfaction* for complex personalized photo retrieval.

These findings indicate that the next frontier in personal multimodal retrieval, especially for photo album scenarios, lies *not only* in establishing stronger unified embedding models, *but also* in developing robust and lightweight agentic reasoning systems capable of traversing the modality gap and resolving the source fusion paradox. We believe that our PHOTOBENCH could serve as the key testbed for this evolution.

In summary, our main contributions are:

- We introduce **PHOTOBENCH**, the first multimodal retrieval benchmark derived from authentic, metadata-rich personal albums. Through *multi-source profiling* for each image, it provides the dense context necessary to evaluate complex reasoning on multi-source personalized information beyond visual matching.

- We propose **intent-driven query synthesis**, which is a *generalized* methodology for personalized multimodal retrieval query generation. It synthesizes narrative yet complex queries rooted in users’ life trajectories, followed by exhaustive ground truth mining for comprehensive evaluation. Moreover, zero-ground-truth queries are also introduced to evaluate the system reliability.
- Experiments on PHOTOBENCH demonstrate that current retrieval models and systems struggle to fulfill the personalized multi-source photo retrieval task. By identifying the **modality gap** and **source fusion paradox**, we point out a critical direction for personalized multimodal retrieval, especially for photo album scenarios, *i.e.*, shifting from unified embedding-centric paradigms to robust and lightweight agentic retrieval systems.

2 Related Work

Multimodal Retrieval Benchmarks. Multimodal retrieval has moved beyond object matching toward semantic understanding. Early benchmarks like MSCOCO [19] and Flickr30k [29] focused on simple matching between visual content and captions. Recent datasets introduce more complexity: Winoground [36] tests compositional reasoning, while INQUIRE [39] evaluates retrieval in large-scale pools. Other works target specific domains, such as Visual News [20] for metadata, VisDial [7] for conversational search, and LSC [10] for lifelogging trajectories. Composed Image Retrieval (CIR) datasets, including Fashion IQ [41] and CIRR [22], further expand the field by using a reference image with text modifications. However, existing benchmarks often focus on visual content rather than the user’s underlying intent. PHOTOBENCH addresses this by mapping complex queries to user motivations in personal photo albums, covering continuous life segments and long-term memory.

Multimodal Representation. Retrieval performance depends on how well models represent data in a latent space. CLIP [30] and SigLIP [48] established the foundation for cross-modal alignment. To improve discriminative power, recent methods use hard negative gradient amplification [43] and smart batch mining [35]. With the rise of generative multimodal large language models (MLLMs), recent works start to train embedding models using MLLMs as backbones. Models like Qwen3-VL [17, 44] and InternVL [3, 23] are now used as powerful encoders through frameworks like VLM2Vec [14, 25] and Rzenembed [12]. Mapping-based methods, such as FiRE [11] and iSEARLE [1], also use MLLMs for textual inversion and context learning [9, 15]. Despite these gains, these embeddings in a unified

latent semantic space often fail to decompose personal queries that involve complex metadata or OCR results [2].

Agentic and Reasoning-based Retrieval. As tasks grow more complex, researchers are moving from static matching toward reasoning-based search. Following frameworks like ReAct [47] and Reflexion [32], agentic retrieval systems solve tasks by calling external tools. This trend includes MMSearch [13], AutoCIR [4] and XR [45], which use multi-agent collaboration for retrieval, and MRA-CIR [38], MM-R1 [18], MMSearch-R1 [42] which employs reasoning agents for open-ended search. Other strategies, such as LDRE [46] and *Reason-before-retrieve* [33], use divergent thinking to clarify ambiguous queries before searching. While these approaches represent the current frontier, they need challenging benchmarks to test their reliability and ability to handle unanswerable questions [16]. PHOTOBENCH provides a unified framework to evaluate both traditional embedding models and newer agentic pipelines.

3 Dataset Construction

Unlike web-scale image collections characterized by isolated snapshots, photo albums are defined by their **ecological validity**: (1) the images are temporally continuous, socially entangled, and deeply personalized, and (2) the user queries are intent-driven and depend on multi-source private contexts. PHOTOBENCH is explicitly designed to capture this contextual depth, distinguishing it from general-purpose multimodal retrieval benchmarks. The construction process is divided into two stages:

- **Album collection and multi-source profiling.** We collect authentic, temporally continuous personal albums and construct a structured, multi-source profile for each image. This process integrates fine-grained visual semantics, high-fidelity spatio-temporal metadata, social cues, and hierarchical event structures.
- **Intent-driven query synthesis.** Rather than relying on static descriptive captions, we synthesize queries by inferring user intentions from their life trajectory. This is followed by a rigorous, expert-verified mining process to ensure exhaustive ground truth recall, alongside the generation of diagnostic zero-ground-truth queries to test system reliability (*i.e.*, rejection capability).

Due to page limitation, we provide all the prompts used for LLM or MLLM generation in Appendix A.

3.1 Album Collection & Multi-Source Profiling

3.1.1 Album Collection. To ensure high ecological validity, PHOTOBENCH is constructed from authentic, temporally continuous photo albums acquired from a diverse demographic pool, spanning varied age groups and professional backgrounds. The collection protocol adheres to two governing policies:

- **Holistic metadata retention.** We posit that photo album retrieval is inextricably linked to non-visual context. Consequently, we prioritize albums with high metadata integrity, ensuring that all collected assets retain their original high-fidelity spatio-temporal signals (*e.g.*, timestamps, GPS coordinates, and device headers) exactly as captured by the source devices.
- **Privacy review with minimal curation.** We purchased complete albums from consenting participants, rather than selectively sampling representative photos. To make PHOTOBENCH publicly releasable, we conducted a privacy screening process

that combines user feedback and expert review. Participants were allowed to flag sensitive content, and experts further removed or masked images containing highly private or identifying information (*e.g.*, confidential documents, personal IDs or other content unsuitable for public release). Beyond this necessary privacy filtering, we intentionally avoided additional manual pruning or aesthetic curation, so that the albums maintain their original characteristics and natural photo distributions.

3.1.2 Multi-Source Profiling. Each collected photo inherently provides its visual content and on-device metadata. Therefore, for each image i , we begin profiling from two native sources, *i.e.*, visual feature and metadata as follows:

- **Visual features \mathcal{V}_i .** Beyond the raw image itself, we use an MLLM (*i.e.*, GPT-4o) to extract and caption the fine-grained visual semantics that are frequently referenced in real queries, including salient objects, human poses, scene composition, and aesthetic attributes.
- **Spatio-temporal metadata \mathcal{M}_i .** We transform low-level metadata into semantic descriptors. Raw GPS coordinates are mapped to semantic places-of-interest (POIs) via reverse geocoding, and timestamps are normalized into human-like temporal tags, *e.g.*, early morning, weekend, and Halloween.

Beyond intrinsic attributes \mathcal{V}_i and \mathcal{M}_i , personal albums are structured by social relations and temporal narratives. We therefore augment the profile with two relational components:

- **Social identity \mathcal{F}_i .** We construct a local social graph for each album via face detection and clustering. Following ego-identification (isolating the album owner), human experts annotate recurring identity clusters with plausible social roles (*e.g.*, spouse, colleague) based on co-occurrence patterns. This produces structured and personalized cues that enable relational references.
- **Temporal event \mathcal{E}_i .** To reconstruct the user’s life trajectory, we perform hierarchical temporal clustering. Photos exhibiting temporal proximity within a definable window form an event cluster. In our implementation, we utilize an adaptive 4-hour window with a minimum cluster size of 3 images. Each cluster is assigned a concise textual summary (*e.g.*, *business dinner at a Japanese restaurant*), providing the necessary temporal context for the subsequent inference of user intention.

With these steps, each image i is associated with a temporally dependent and multi-source profile, represented as:

$$\mathcal{P}_i = \{\mathcal{V}_i, \mathcal{M}_i, \mathcal{F}_i, \mathcal{E}_i\}, \quad (1)$$

which serves as the structured data foundation for the subsequent intent-driven query synthesis stage.

3.2 Intent-Driven Query Synthesis

Authentic retrieval requests in personal archives are rarely simple visual descriptions; they are anchored in specific memory traces and grounded in heterogeneous, personalized contexts. To emulate this complexity, we employ an intent-driven query synthesis pipeline. Specifically, we construct each query by starting with an anchor image i and its profile \mathcal{P}_i . We first infer the *user intention* behind the image by analyzing the user’s event trajectory, and then

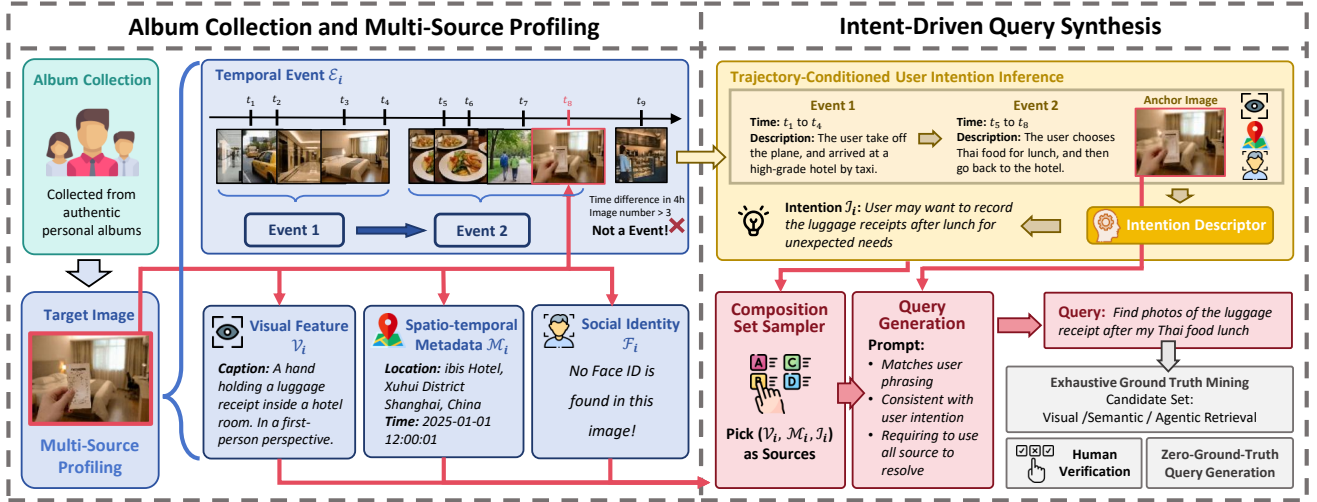


Figure 1: The illustration of the dataset construction pipeline for PHOTOBENCH.

synthesize a natural query by composing information from multiple profile dimensions. Crucially, to ensure robust evaluation, we conduct exhaustive ground truth mining and expert verification to establish dense ground truth. Furthermore, we also generate some zero-ground-truth queries that have no ground truth images to evaluate the system’s rejection capability.

3.2.1 Trajectory-Conditioned User Intention Inference. A single photo is often only a snapshot of a broader activity, and its purpose is best understood in the context of evolving events. For each image i , we infer an intention descriptor \mathcal{I}_i by conditioning on its profile \mathcal{P}_i and the textual summaries of preceding events:

$$\mathcal{I}_i = \text{MLLM}(\mathcal{P}_i, [\mathcal{E}_j]_{j \leq i}), \quad (2)$$

where $[\mathcal{E}_j]_{j \leq i}$ denotes the chronological trajectory of event summaries that occur earlier in the album timeline. The output \mathcal{I}_i is a concise, human-like description of the user’s potential intention (e.g., *to keep the dinner receipt during a business trip*). In this way, we encourage the model to exploit trajectory context rather than relying on single-image captioning.

3.2.2 Query Synthesis via Multi-source Composition. Given the inferred intention \mathcal{I}_i and the profile \mathcal{P}_i , we synthesize diverse queries for image i by composing multiple available information sources. Specifically, we sample a composition set:

$$\mathcal{H} \subseteq \{\mathcal{V}_i, \mathcal{M}_i, \mathcal{F}_i, \mathcal{I}_i\}, \quad (3)$$

and prompt an LLM/MLLM to generate a natural-language query q that: (1) mirrors realistic user phrasing, (2) remains logically consistent with \mathcal{I}_i , and (3) strictly requires the intersection of sources in \mathcal{H} to resolve ambiguity in a dense gallery. This mechanism yields narrative, personalized queries that closely approximate human memory retrieval patterns (see Appendix G.4 for examples).

3.2.3 Exhaustive Ground Truth Mining and Verification. In ecological photo retrieval, a single query often corresponds to multiple valid targets (e.g., burst shots, near-duplicates, or thematically

linked events) among numerous hard distractors. To ensure PHOTOBENCH supports rigorous recall evaluation, we move beyond the single anchor image i and perform *exhaustive ground truth mining* for the synthesized query q . Concretely, we construct a candidate set by combining complementary retrieval methods:

- **Visual retrieval:** Top- K neighbors based on visual embedding similarity, capturing perceptually identical near-duplicates.
- **Semantic retrieval:** Top- K neighbors using text embeddings over query q and caption from \mathcal{P}_i , to capture the semantically relevant but visually distinct photos.
- **Agentic multi-tool retrieval:** A rigorous agentic pipeline that filters the album using metadata, identity, and event constraints to uncover valid matches that embedding models might miss.

Empirically, we set $K = 50$, which effectively covers the valid solution space. Finally, human experts manually review every instance in the candidate pool to annotate all valid positives and filter out ambiguous or ill-posed queries. This combination of automated exhaustive mining and human verification ensures that our PHOTOBENCH provides a **comprehensive ground truth set**, distinguishing it from web-scale datasets where labels are often sparse and incomplete.

3.2.4 Zero-Ground-Truth Query Generation. To evaluate a retrieval system’s rejection capability to resist user hallucination, we simulate “false memory” scenarios where users query for plausible but non-existent images (e.g., a specific person at an event they did not attend). We generate a set of *zero-ground-truth (Zero-GT)* queries using counterfactual synthesis. Detailed generation protocols are provided in Appendix A.4.

4 Dataset Statistics

In this section, we present a statistical overview of PHOTOBENCH, focusing on its overall characteristics and our proposed source-aware taxonomy. We also provide the detailed dataset statistics and distribution analysis in Appendix C.

4.1 Dataset Overview

Following the ecological construction protocol outlined in Section 3, PHOTOBENCH consists of 3,582 images sampled from three authentic, personal albums, paired with 1,188 bilingual queries (Chinese and English). Unlike web-scraped datasets characterized by sparse labels, PHOTOBENCH offers *dense, exhaustive ground truth* within a continuous life-logging context. It exhibits three critical characteristics designed to test complex retrieval capabilities:

- **Spatio-Temporal Fidelity:** 83.4% of images retain valid high-precision GPS and timestamp metadata. The data covers a temporal range from 2018 to 2025, capturing diverse settings from major metropolitan areas in China to international POIs across East and Southeast Asia. This is essential for evaluating the retrieval systems' ability to perform rigorous spatio-temporal filtering, which is often untested in metadata-stripped web datasets.
- **Social-Relational Density:** The albums collectively feature 20 distinct recurring individuals, with 25.1% of images classified as portraits. This density enables the evaluation of long-tail social identity recognition and relationship-based retrieval.

We provide per-album statistical analysis in Appendix C.1.

4.2 Source-Aware Query Taxonomy

To enable precise failure attribution (*e.g.*, distinguishing visual failures from reasoning failures), we introduce a *Source-Aware Query Taxonomy*. Curated via expert annotation, this taxonomy classifies queries based on the *necessary and sufficient* information sources required to resolve the user query for image retrieval. We define three atomic information dimensions:

- **Vision (S_V):** Queries resolvable solely through visual perception, involving physical entities, scene aesthetics, or composition (*e.g.*, *photo of red flowers*).
- **Metadata (S_M):** Queries grounded in spatio-temporal context, requiring access to timestamp or geolocation logs (*e.g.*, *photos from Tokyo in 2025*).
- **Face (S_F):** Queries targeting specific social identities or relationships, requiring face recognition or social graph access (*e.g.*, *photo of my sister*).

Real-world intents are often entangled. Queries requiring multiple information sources are classified into **compositional categories** (*i.e.*, S_{VM} , S_{VF} , S_{MF} , and S_{VMF}). For instance, S_{VM} denotes a query requiring both visual recognition and metadata filtering. Crucially, this classification is strict and non-overlapping. A query assigned to a composite category (*e.g.*, S_{VM}) is *not* double-counted under S_V or S_M . This mutual exclusivity provides a rigorous foundation for evaluating retrieval systems' ability to process and fuse multiple information sources.

Figure 2 presents the query distribution in terms of both ground-truth count and source-aware taxonomy. The ground truth distribution exhibits a long-tail characteristic, challenging systems to handle both specific needle-in-a-haystack retrieval and broader event-level recall. Notably, a significant proportion of queries fall into composite categories (*e.g.*, S_{VM} , S_{VMF}), highlighting that the primary challenge in personal retrieval is not merely visual matching, but the *cross-modal fusion* of heterogeneous signals.

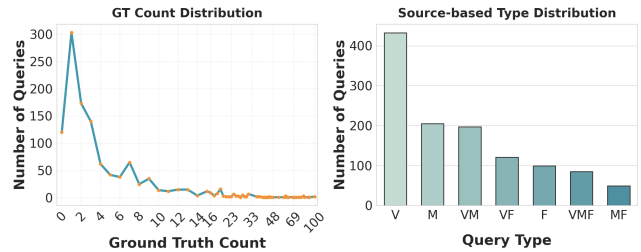


Figure 2: The query distribution w.r.t. ground-truth count (left) and source-aware taxonomy (right) in PHOTOBENCH.

5 Experiment

PHOTOBENCH evaluates retrieval systems in a personalized, intent-driven context that differs substantially from static, context-isolated web benchmarks. In this section, we benchmark a diverse spectrum of retrieval paradigms to establish rigorous baselines for the research community. We report primary results on the Chinese version of PHOTOBENCH. We provide the case studies of various failure modes in PHOTOBENCH in Appendix G due to the page limitation.

5.1 Evaluated Models and Systems

We evaluate two distinct architectural families: *Unified Embedding Models* (single-step matching) and *Hybrid Retrieval Systems* (multi-step, tool-augmented reasoning).

5.1.1 Unified Embedding Models. These methods map images and queries into a shared latent space for similarity-based retrieval. We categorize them into two subgroups:

- **Multimodal embedding models** that directly embed visual and textual inputs. We select representative baselines across varying scales, including dual-encoder models (*i.e.*, CLIP [30], SigLIP2-base/giant [37]) and VLM-based dense retrievers (*i.e.*, VLM2Vec [14], B3_Qwen2_7B [34], Qwen3-VL-Embedding-2B/8B [17], Ops-MM-embedding-v1 [28], RzenEmbed-v2-7B [12] and QQMM-embed-v2 [43]).
- **Caption-based text embedding pipelines** that first convert images to textual captions using GPT-4o and then perform text-to-text retrieval. For the textual encoder, we employ BGE-M3 [2], multilingual-E5 series [40], and Qwen3-Embedding series [49].

5.1.2 Hybrid Retrieval Systems. These systems utilize compositional reasoning or heuristic logic to combine multiple retrievers and signals (*e.g.*, visual similarity, metadata constraints), typically returning a *variable-length* result set.

- **Tool-based agentic systems.** To evaluate the potential of LLM in resolving complex retrieval intents, we implement a *ReAct-style agent* [47] instantiated with various SOTA LLM backbones capable of tool invocation, including ToolACE-2-Llama-3.1-8B [21], Qwen3-8B/32B [44], DeepSeek-V3 [8], Qwen3-235B-A22B [44], GPT-4o [26], OpenAI-o3 [27], Claude-Sonnet-4-5 [6], and Claude-Opus-4-5 [5]. To strictly align with the information sources defined in Section 4.2, we equip the agent with following tools:

- **Vector search engine** (T_V) performs semantic visual retrieval over a FAISS-indexed embedding space. We adopt RzenEmbed-v2-7B [12] as the encoder, as it demonstrates superior performance among unified embedding models (see Section 5.3).
- **Metadata filter** (T_M) executes hard filtering based on spatio-temporal constraints (timestamps, GPS coordinates, and POIs).
- **Face search engine** (T_F) resolves identity constraints and social references using face clusters and annotated role tags.
- **Set composition tool** (T_S) enables the agent to perform logical set operations (intersection/union/difference) over outputs from different tools to synthesize the final prediction.
- **Real-world mobile gallery systems.** To contextualize academic findings against industrial standards, we evaluate the native gallery search performance of six mainstream flagship smartphones, covering the three dominant ecosystems: iOS, Android and HarmonyOS. We strictly follow a black-box evaluation protocol: albums are imported into the native gallery, indexed by the on-device engine, and queried via an automated scripting tool. To focus the evaluation on the representative capabilities of mature commercial systems rather than the specific performance of individual brands, we have anonymized the devices as Phone A to Phone F. The detailed evaluation protocol is in Appendix F

5.2 Evaluation Metrics

PHOTOBENCH presents two evaluation challenges: (1) it supports one-to-many matches with variable ground truth sizes, and (2) it includes zero-ground-truth (Zero-GT) queries that require system abstention. Hence, we employ two complementary metric families:

- **Top-K Ranking Metrics.** Designed for embedding models that output *fixed-length lists*. We report Recall@K and NDCG@K with $K \in \{1, 5, 10, 20\}$, covering the spectrum from best hit to broad shortlists.
- **Set-Based Metrics.** Only suitable for hybrid retrieval systems (*i.e.*, Agents and Phones) that return *variable-length sets*. We evaluate performance across two query types:
 - **Normal Query.** We report standard Precision, Recall, and F1 to measure the accuracy of the returned image set against the comprehensive ground truth set.
 - **Zero-GT Query.** To measure systems' ability to correctly abstain (reject) when no relevant photo exists, we report Reject-Precision, Reject-Recall, and Reject-F1. Here, Reject-Recall measures the proportion of Zero-GT queries correctly identified as empty, while Reject-Precision measures the reliability of an empty response. Formal definitions are provided in Appendix B.2.

5.3 Main Results

Table 2 presents the comparative performance of unified embedding models and tool-based agentic systems across standard top-k ranking metrics. We observe three key trends:

- **Visual-Linguistic Compression Loss.** Caption-based text embedding pipelines consistently underperform multimodal embedding models. Despite the augmentation of caption with structured metadata (*e.g.*, time and location), the performance gap persists. This suggests a fundamental *information bottleneck*: converting dense, fine-grained visual signals into discrete textual

intermediates would lead to irreversible semantic loss, limiting the performance of text-based retrieval.

- **Superiority of Explicit Tool Orchestration.** Tool-based agentic systems significantly outperform unified embedding models. This validates that personal album retrieval is not merely a visual matching problem but a *multi-source constrained* problem. By explicitly orchestrating specialized tools, agents effectively bypass the limitations of monolithic embedding spaces, leveraging heterogeneous signals to resolve complex user intents.
- **Scaling Laws Hold for Both Paradigms.** For embedding models, larger backbones yield better semantic alignment. Crucially, for agentic systems, performance gains correlate with both the backbone size and tool-calling capability (*e.g.*, Qwen3-235B vs. Qwen3-8B). This indicates that retrieval quality in this regime is limited not just by visual perception, but by the *planning capacity* required to decompose and execute multi-step queries.

Table 3 benchmarks the agentic retrieval systems against commercial mobile gallery systems using set-oriented metrics, separately on normal and zero-GT queries. This comparison reveals a critical trade-off between reasoning capability and system reliability:

- **Retrieval Ceiling (Normal Query).** Agentic retrievers consistently achieve higher set-level F1 scores compared to all evaluated mobile systems on normal queries. Potentially due to the on-device resource constraints, commercial retrieval engines usually prefer lightweight retrieval methods and thereby struggle with the entangled, intent-driven queries characteristic of PHOTOBENCH. Although costly, agents define a significantly higher performance ceiling for complex retrieval with their ability to synthesize evidence from multiple sources.
- **Reliability & Abstention (Zero-GT Query):** The trend reverses on rejection metrics. Mobile systems demonstrate superior Reject-Recall, reflecting a conservative engineering design optimized for precision (preferring no result over a wrong one). In contrast, agentic systems exhibit a tendency towards *Retrieval Hallucination*, forcing matches for non-existent queries. This highlights a pivotal challenge for future research: **beyond maximizing recall, agentic retrievers must develop calibrated proactive abstention mechanisms to operate reliably in open-world environments.**

5.4 In-Depth Analysis

To decompose the performance dynamics of each retrieval paradigm, we analyze the retrieval behaviors through the lens of our *Source-Aware Query Taxonomy* introduced in Section 4.2. We derive the following key insights for the three retrieval paradigms.

5.4.1 Analysis of Unified Embedding Models. To diagnose the intrinsic limitations of unified embedding models, we analyze the averaged performance of three categories (*i.e.*, agentic systems, multimodal embedding, and caption-based text embedding) across source-based query types defined in our taxonomy. We report Recall@10 performance in Table 4 and derive two critical findings:

- **Modality Gap.** Unified embedding models exhibit a fundamental bias toward visual signals. While they achieve strong performance on purely visual queries (S_V), their efficacy collapses on queries requiring explicit metadata (S_M) or identity verification

Table 2: The retrieval performance on PHOTOBENCH using top- k ranking metrics. We report Recall@ K (R@ K) and NDCG@ K (N@ K) averaged over all albums. Best result of each category is in bold, and the second best is underlined.

Model	Size (B)	Chinese							English								
		R@1	R@5	R@10	R@20	N@1	N@5	N@10	N@20	R@1	R@5	R@10	R@20	N@1	N@5	N@10	N@20
<i>Multimodal Embedding Models</i>																	
clip-ViT-B-32-multilingual-v1	0.14	1.2	4.1	6.1	8.8	3.2	4.0	4.7	5.5	10.7	25.5	33.1	41.3	24.5	25.6	27.9	30.3
siglip2-base-patch16-224	0.38	16.4	33.7	40.0	47.3	33.1	34.6	36.0	38.2	19.8	39.9	46.7	53.1	40.2	41.5	42.9	44.7
siglip2-giant-opt-patch16-256	1.88	20.8	40.5	47.6	54.5	42.0	42.4	44.1	46.0	<u>23.8</u>	45.1	50.7	56.9	47.5	48.1	48.8	50.5
VLM2Vec	8.29	23.1	44.4	52.4	60.0	46.0	47.0	48.9	51.3	22.0	43.3	51.1	58.1	43.0	44.9	46.9	49.1
B3_Qwen2_7B	8.29	20.9	41.4	49.9	57.1	41.9	43.6	45.6	47.8	21.1	42.4	50.1	55.9	42.3	43.7	45.7	47.4
Qwen3-VL-Embedding-2B	2.13	22.7	42.5	50.6	58.2	44.6	45.4	47.4	49.5	21.6	40.3	48.1	55.9	42.9	43.2	45.1	47.6
Qwen3-VL-Embedding-8B	8.14	24.9	46.2	53.0	59.2	49.7	49.7	50.9	52.6	<u>23.8</u>	45.2	51.9	58.4	46.8	47.9	49.2	50.9
Ops-MM-embedding-v1	8.29	25.8	48.7	56.6	63.7	49.8	51.7	53.5	55.5	25.5	<u>48.3</u>	<u>56.0</u>	<u>63.4</u>	50.9	51.8	<u>53.2</u>	<u>55.3</u>
RzenEmbed-v2-7B	8.29	27.2	<u>49.9</u>	58.0	<u>65.1</u>	54.1	54.3	56.0	57.9	25.6	48.5	56.5	64.1	<u>50.8</u>	51.8	<u>53.7</u>	55.8
QQMM-embed-v2	8.29	<u>26.6</u>	50.0	<u>57.8</u>	65.4	<u>52.3</u>	<u>53.7</u>	<u>55.4</u>	<u>57.6</u>	25.1	47.8	55.9	63.6	49.3	50.6	52.6	54.9
<i>Caption-based Text Embedding Pipelines</i>																	
multilingual-e5-small	0.12	21.6	37.5	42.8	48.8	40.7	39.6	40.7	42.5	19.3	35.6	41.6	47.5	37.1	37.1	38.3	40.0
multilingual-e5-base	0.28	21.8	38.1	44.8	51.9	41.6	40.5	42.2	44.3	20.8	37.7	44.3	50.4	39.0	39.3	41.0	42.8
multilingual-e5-large	0.56	24.2	40.6	47.1	54.6	46.3	44.7	45.9	48.0	20.4	38.1	45.4	50.8	39.7	40.2	42.1	43.5
bge-m3	0.57	23.0	41.6	48.5	56.6	43.8	44.5	46.0	48.5	20.8	38.1	44.7	51.5	41.9	40.6	42.0	43.8
Qwen3-Embedding-0.6B	0.60	24.0	42.0	48.4	54.9	45.9	45.5	46.8	<u>48.6</u>	22.2	39.3	46.1	52.5	42.0	41.7	43.1	45.0
Qwen3-Embedding-4B	4.00	25.6	<u>44.5</u>	<u>51.6</u>	57.9	49.1	48.3	49.8	51.4	<u>24.0</u>	<u>42.3</u>	<u>49.2</u>	55.0	46.1	<u>45.2</u>	<u>46.7</u>	<u>48.2</u>
Qwen3-Embedding-8B	7.60	<u>25.4</u>	44.8	51.7	<u>57.8</u>	<u>48.3</u>	<u>48.2</u>	<u>49.7</u>	51.2	24.3	43.0	49.2	<u>54.8</u>	<u>46.0</u>	45.9	47.0	48.5
<i>Tool-based Agentic Systems</i>																	
ToolACE-2-Llama-3.1-8B	8.00	21.3	44.0	47.7	51.2	48.8	50.9	50.2	50.7	23.0	43.5	46.4	48.2	49.4	49.4	47.7	47.4
Qwen3-8B	8.00	14.5	51.0	60.4	64.1	35.0	53.5	56.4	56.4	14.2	51.2	62.7	66.0	34.1	55.7	58.8	59.3
Qwen3-32B	32.8	28.3	54.1	62.5	64.5	63.6	63.0	63.5	62.4	27.2	54.5	<u>62.7</u>	66.3	59.6	61.5	61.9	62.0
DeepSeek-v3	671	26.8	51.6	60.1	62.4	59.6	59.9	61.0	60.6	24.9	49.4	57.8	60.9	55.5	56.5	57.7	57.8
Qwen3-235B-A22B	235	31.0	60.8	67.0	69.6	<u>70.0</u>	71.4	72.0	71.8	27.7	55.9	60.9	62.8	63.6	65.6	65.7	65.2
GPT-4o	Closed	28.0	53.1	58.5	60.3	60.3	61.1	60.5	59.5	27.6	54.3	60.5	62.3	60.9	61.9	61.7	61.0
OpenAI-o3	Closed	<u>31.2</u>	59.5	<u>68.7</u>	<u>71.4</u>	70.2	<u>69.8</u>	<u>70.6</u>	<u>69.9</u>	<u>29.2</u>	<u>58.5</u>	68.2	71.1	<u>67.2</u>	67.6	68.4	67.9
Claude-Sonnet-4-5	Closed	30.5	<u>60.4</u>	69.5	73.1	69.0	69.7	70.3	70.0	30.4	58.9	<u>68.1</u>	<u>70.4</u>	67.3	<u>67.5</u>	<u>68.3</u>	<u>67.6</u>
Claude-Opus-4-5	Closed	32.1	60.6	<u>68.7</u>	71.7	69.8	69.9	70.3	<u>69.9</u>	28.7	58.1	66.7	69.0	65.2	66.7	67.3	66.5

Table 3: The retrieval performance on PHOTOBENCH using set-based metrics. Best result of each category is in bold, while the second best is underlined. P , R , $Rej-P$, $Rej-R$ and $Rej-F1$ denote Precision, Recall, $F1$, Rej -Precision, Rej -Recall and Rej - $F1$, respectively.

System	Normal Query			Zero-GT Query		
	P	R	F1	Rej-P	Rej-R	Rej-F1
<i>Real-world Mobile Gallery Systems</i>						
Phone A	22.8	47.3	25.6	18.2	73.2	29.1
Phone B	16.0	17.2	14.4	12.4	<u>80.5</u>	21.5
Phone C	33.7	<u>50.1</u>	34.4	20.1	48.8	28.5
Phone D	34.9	47.7	34.5	<u>25.5</u>	79.7	<u>38.6</u>
Phone E	40.9	43.3	<u>38.3</u>	20.9	82.3	33.4
Phone F	<u>37.6</u>	65.4	40.2	36.5	63.4	46.3
<i>Tool-based Agentic Systems</i>						
ToolACE-2	38.3	54.7	39.0	15.1	35.0	<u>21.1</u>
Qwen3-8B	37.6	68.1	41.0	16.8	16.7	16.7
Qwen3-32B	39.6	66.3	41.4	16.7	25.8	20.3
DeepSeek-v3	38.5	66.2	40.7	11.8	10.0	10.8
Qwen3-235B-A22B	50.8	71.6	51.9	14.3	6.7	9.1
GPT-4o	45.4	65.3	46.4	13.8	17.5	15.4
OpenAI-o3	44.6	<u>75.2</u>	48.0	34.5	<u>33.3</u>	33.9
Claude-Sonnet-4.5	43.7	78.3	47.9	14.3	8.3	10.5
Claude-Opus-4.5	<u>46.9</u>	74.7	<u>50.5</u>	<u>18.2</u>	13.3	15.4

(S_F). The agentic system outperforms embedding models by vast

Table 4: Recall@10 performance decomposition by source-aware query types. $\Delta(A-M)$ and $\Delta(A-T)$ denote performance gaps between agents and multimodal and caption-based text embedding models, respectively.

Type	Agent(A)	Multimodal(M)	Text(T)	$\Delta(A-M)$	$\Delta(A-T)$
S_V	71.1	72.3	75.0	-1.2	-3.8
S_M	57.9	7.2	7.9	+50.8	+50.1
S_F	75.1	11.7	8.4	+63.4	+66.7
S_{VM}	63.4	63.4	65.5	+0.0	-2.1
S_{VF}	40.1	52.6	51.0	-12.4	-10.9
S_{MF}	60.2	12.0	11.2	+48.2	+49.0
S_{VMF}	37.5	51.4	46.5	-13.9	-9.0

margins in these categories. This confirms that current multimodal embeddings function primarily as *visual similarity calculators*, lacking the capacity to encode precise spatio-temporal or social identity constraints in their latent space.

- **Visual-Anchor Effect.** Counterintuitively, embedding models remain competitive (often superior) on compositional queries containing visual terms (*i.e.*, S_{VM} , S_{VF} , S_{VMF}), despite their demonstrated inability to process the non-visual components (M and F). We attribute this to the *visual-anchor effect*: in many compositional queries, the non-visual constraint is highly correlated with a distinctive visual cue (*e.g.*, a “birthday” event implies the

Table 5: Tool ablation study on the best agentic system with Qwen3-235B-A22B. F1 scores are reported across query types as different types of tools are incrementally enabled. Note that the set composition tool (T_S) is always active.

Tools	S_V	S_M	S_F	S_{VM}	S_{VF}	S_{MF}	S_{VMF}
T_V	30.5	2.6	8.7	31.4	32.1	6.1	35.1
$T_V + T_M$	32.3	54.7	12.9	34.1	33.2	25.5	33.4
$T_V + T_F$	32.2	3.3	69.0	29.7	26.8	30.1	25.4
$T_V + T_M + T_F$	36.9	69.7	90.1	44.7	30.1	76.8	32.5

visual presence of a “cake”). Embedding models exploit these visual anchors to retrieve correct targets via appearance matching without truly resolving the underlying metadata or identity logic. In contrast, agentic systems act as strict logical reasoners and may fail if a specific tool misses a target, leading to lower recall on these “visually solvable” compositional queries.

5.4.2 Analysis of Agentic Retrieval Systems. We conduct a tool ablation study to investigate the mechanism behind the agent’s performance profile, specifically its strength on metadata/face queries versus its struggle on composite visual queries. Using the strongest agent backbone (Qwen3-235B-A22B), we systematically enable different combinations of the Vector Search (T_V), Metadata Filter (T_M), and Face Engine (T_F) tools. Table 5 reports the set-based F1 score across query types, from which we draw two key insights:

- **Decisive Role of Explicit Tool Access.** Performance improvements are strictly source-aligned, confirming that the agent’s capability is architectural rather than emergent. Enabling the Metadata Filter (T_M) yields a massive gain on S_M queries (from 2.6 to 54.7), just as the Face Engine (T_F) unlocks S_F performance (from 8.7 to 69.0). Furthermore, visual grounding remains essential for disambiguation: introducing T_V alongside non-visual tools is critical for composite queries like S_{VMF} , ensuring that the agent can visually pinpoint the correct target among dense near-duplicates that satisfy the metadata constraints.
- **Source Fusion Paradox.** Crucially, simply maximizing tool availability does not guarantee performance improvement. For the most complex queries (S_{VMF}), enabling the full tool suite ($T_V + T_M + T_F$) yields a lower F1 score (32.5) than using the visual tool alone (T_V at 35.1). This counterintuitive degradation reveals the *Source Fusion Paradox*: as the decision space expands, the agent increasingly struggles with *tool orchestration*. It often generates suboptimal execution plans or applies overly aggressive set intersections (e.g., combining a noisy face retrieval set with a precise time window), leading to the erroneous pruning of valid results. In this sense, the intrinsic reasoning and tool-calling capabilities are the major bottleneck of agentic retrieval systems.

5.4.3 Analysis of Mobile Gallery Systems. We analyze the performance degradation of six commercial gallery systems (Phones A–F) alongside our best agentic model. Table 6 reports the average F1 scores across single, dual, and triple-source queries, along with the performance change (Δ) between complexity levels. We highlight two divergent system behaviors:

- **Universal Degradation via Constraint Fusion ($\Delta_{2-1} < 0$).** The challenge of fusing heterogeneous sources is universal. When

Table 6: We report F1 scores of the best agent (Qwen3-235B-A22B) and mobile gallery systems as query complexity increases from single- to dual- and triple-source queries. Δ values indicate the performance degradation, exposing the Source Fusion Paradox in commercial engines.

Type	Agent (Best)	Pho.A	Pho.B	Pho.C	Pho.D	Pho.E	Pho.F
S_V	37.6	33.2	20.5	34.6	34.1	40.6	36.4
S_M	72.3	39.8	17.9	67.5	52.6	75.1	76.7
S_F	93.4	1.8	1.1	1.7	6.7	0.0	10.3
Avg.	63.5	28.8	15.0	40.4	31.7	45.2	46.3
S_{VM}	45.7	20.0	10.9	31.7	32.2	38.3	40.4
S_{VF}	30.9	15.1	7.2	22.7	25.9	20.8	22.2
S_{MF}	80.5	13.4	3.0	7.3	18.8	4.8	34.5
Avg.	52.4	16.2	7.1	20.6	25.6	21.3	32.4
S_{VMF}	33.9	13.5	9.1	23.8	24.5	27.7	22.4
Δ_{2-1}	-17.6	-43.9	-52.7	-49.1	-19.0	-52.9	-30.1
Δ_{3-2}	-35.2	-16.3	+28.8	+15.7	-4.4	+30.1	-30.8
Δ_{3-1}	-46.6	-53.1	-39.1	-41.1	-22.6	-38.7	-51.6

transitioning from single-source to dual-source queries (e.g., adding a time constraint to a visual search), both agentic and commercial systems suffer significant performance decay. This confirms that the *Source Fusion Paradox* is not an artifact of our agentic implementation, but a fundamental reliability gap in current retrieval architectures when handling conjoint constraints.

- **Rebound via Visual-Anchor Effect ($\Delta_{3-2} > 0$).** A distinct anomaly occurs at the triple-source level (S_{VMF}). While the agent continues to degrade monotonically, several commercial systems (Phones B, C, and E) exhibit a performance rebound, *improving* by +15% to +30% compared to dual-source queries. We attribute this to the same *Visual Anchor Effect* observed in Section 5.4.1. These commercial engines likely prioritize visual similarity scores over strict metadata or identity filtering. When a visual term is reintroduced in a S_{VMF} query, the system latches onto this visual anchor, effectively bypassing the failed non-visual logic (S_{MF}) to salvage recall. Thus, this performance rebound is deceptive; it reflects a heuristic retreat to visual perception rather than a successful fusion of multi-source constraints.

6 Conclusion and Future Direction

We introduce PHOTOBENCH, a diagnostic benchmark that shifts the evaluation of mobile photo retrieval from visual matching to multi-source, intent-driven reasoning. By reconstructing the dense entanglement of visual semantics, spatial-temporal metadata, social identity, and temporal events established in authentic albums, PHOTOBENCH exposes critical limitations of existing retrieval models and systems that remain hidden in context-isolated web datasets. Our investigation reveals two defining challenges for the research community like the modality gap and source fusion paradox. Ultimately, PHOTOBENCH suggests that the future of personal multi-modal retrieval, especially for photo album scenarios, lies beyond establishing stronger unified embedding models. It requires a fundamental transition towards robust agentic reasoning systems capable of precise constraint satisfaction, proactive abstention, and the reliable fusion of heterogeneous, personalized signals.

References

- [1] Lorenzo Agnolucci, Alberto Baldradi, Marco Bertini, and Alberto Del Bimbo. 2024. iSEARLE: Improving Textual Inversion for Zero-Shot Composed Image Retrieval. *arXiv preprint arXiv:2405.02951* (2024).
- [2] Jianlv Chen, Shitao Xiao, Peitian Zhang, Kun Luo, Defu Lian, and Zheng Liu. 2024. Bge m3-embedding: Multi-lingual, multi-functionality, multi-granularity text embeddings through self-knowledge distillation. *arXiv preprint arXiv:2402.03216* 4, 5 (2024).
- [3] Zhe Chen, Jiannan Wu, Wenhai Wang, Weijie Su, Guo Chen, Sen Xing, Muyan Zhong, Qinglong Zhang, Xizhou Zhu, Lewei Lu, et al. 2024. Internvl: Scaling up vision foundation models and aligning for generic visual-linguistic tasks. In *Proceedings of the IEEE/CVF conference on computer vision and pattern recognition*. 24185–24198.
- [4] Zhangtao Cheng, Yuhao Ma, Jian Lang, Kumpeng Zhang, Ting Zhong, Yong Wang, and Fan Zhou. 2025. Generative Thinking, Corrective Action: User-Friendly Composed Image Retrieval via Automatic Multi-Agent Collaboration. In *Proceedings of the 31st ACM SIGKDD Conference on Knowledge Discovery and Data Mining (KDD)*. 334–344.
- [5] Claude. 2025. Claude Opus 4.5. <https://www-cdn.anthropic.com/bf10f64990cfd0ba858290be7b8cc6317685f47.pdf>
- [6] Claude. 2025. Claude Sonnet 4.5. <https://www.anthropic.com/claude/sonnet>
- [7] Abhishek Das, Satwik Kottur, Khushi Gupta, Avi Singh, Deshraj Yadav, José MF Moura, Devi Parikh, and Dhruv Batra. 2017. Visual dialog. In *Proceedings of the IEEE conference on computer vision and pattern recognition*. 326–335.
- [8] DeepSeek-AI, Aixin Liu, Bei Feng, Bing Xue, Bingxuan Wang, Bochao Wu, Chengda Lu, Chenggang Zhao, Chengqi Deng, Chenyu Zhang, Chong Ruan, Damai Dai, Daya Guo, Dejian Yang, Deli Chen, Dongjie Ji, Erhang Li, Fangyun Lin, Fucang Dai, Fuli Luo, Guangbo Hao, Guanting Chen, Guowei Li, H. Zhang, Han Bao, Hanwei Xu, Haocheng Wang, Haowei Zhang, Honghui Ding, Huaqian Xin, Huazuo Gao, Hui Li, Hui Qu, J. L. Cai, Jian Liang, Jianzhong Guo, Jiaqi Ni, Jiashi Li, Jiawei Wang, Jin Chen, Jingchang Chen, Jingyang Yuan, Junjie Qiu, Junlong Li, Junxiao Song, Kai Dong, Kai Hu, Kaige Gao, Kang Guan, Kexin Huang, Kuai Yu, Lean Wang, Lecong Zhang, Lei Xu, Leyi Xia, Liang Zhao, Litong Wang, Liyue Zhang, Meng Li, Miaojun Wang, Mingchuan Zhang, Minghua Zhang, Minghui Tang, Mingming Li, Ning Tian, Panpan Huang, Peiyi Wang, Peng Zhang, Qiancheng Wang, Qihao Zhu, Qinyu Chen, Qiusi Du, R. J. Chen, R. L. Jin, Ruiqi Ge, Ruisong Zhang, Ruizhe Pan, Runji Wang, Runxin Xu, Ruoyu Zhang, Ruyi Chen, S. S. Li, Shanghao Lu, Shangyan Zhou, Shanhuan Chen, Shaoqing Wu, Shengfeng Ye, Shengfeng Ye, Shirong Ma, Shiyu Wang, Shuang Zhou, Shuiping Yu, Shunfeng Zhou, Shuting Pan, T. Wang, Tao Yun, Tian Pei, Tianyu Sun, W. L. Xiao, Wangding Zeng, Wanji Zhao, Wei An, Wen Liu, Wenfeng Liang, Wenjun Gao, Wenqin Yu, Wentao Zhang, X. Q. Li, Xiangyue Jin, Xianzu Wang, Xiao Bi, Xiaodong Liu, Xiaohan Wang, Xiaojin Shen, Xiaokang Chen, Xiaokang Zhang, Xiaosha Chen, Xiaotao Nie, Xiaowen Sun, Xiaoxiang Wang, Xin Cheng, Xin Liu, Xin Xie, Xingchao Liu, Xingkai Yu, Xinnan Song, Xinxia Shan, Xinyi Zhou, Xinyu Yang, Xinyuan Li, Xuecheng Su, Xuheng Lin, Y. K. Li, Y. Q. Wang, Y. X. Wei, Y. X. Zhu, Yang Zhang, Yanhong Xu, Yanhong Xu, Yanping Huang, Yao Li, Yao Zhao, Yaofeng Sun, Yaohui Li, Yaohui Wang, Yi Yu, Yi Zheng, Yichao Zhang, Yifan Shi, Yiliang Xiong, Ying He, Ying Tang, Yishi Piao, Yisong Wang, Yixuan Tan, Yiyang Ma, Yiyuan Liu, Yongqiang Guo, Yu Wu, Yuan Ou, Yuchen Zhu, Yudian Wang, Yue Gong, Yuheng Zou, Yujia He, Yukun Zha, Yunfan Xiong, Yuxian Ma, Yuting Yan, Yuxiang Luo, Yuxiang You, Yuxuan Liu, Yuyang Zhou, Z. F. Wu, Z. Z. Ren, Zehui Ren, Zhangli Sha, Zhe Fu, Zhean Xu, Zhen Huang, Zhen Zhang, Zhenda Xie, Zhengyan Zhang, Zhewen Hao, Zhibin Gou, Zhicheng Ma, Zhigang Yan, Zhihong Shao, Zhipeng Xu, Zhiyu Wu, Zhongyu Zhang, Zhuoshu Li, Zihui Gu, Zijia Zhu, Zijun Liu, Zilin Li, Ziwei Xie, Ziyang Song, Ziyi Gao, and Zizheng Pan. 2025. DeepSeek-V3 Technical Report. *arXiv:2412.19437 [cs.CL]* <https://arxiv.org/abs/2412.19437>
- [9] Geonmo Gu, Sanghyuk Chun, Wonjae Kim, Yoohoon Kang, and Sangdoon Yun. 2024. Language-only Training of Zero-shot Composed Image Retrieval. In *Proceedings of the IEEE/CVF Conference on Computer Vision and Pattern Recognition (CVPR)*.
- [10] Cathal Gurrin, Björn Þór Jónsson, Duc Tien Dang Nguyen, Graham Healy, Jakob Lokoc, Liting Zhou, Luca Rossetto, Minh-Triet Tran, Wolfgang Hürst, Werner Bailer, et al. 2023. Introduction to the sixth annual lifelog search challenge, LSC'23. In *Proceedings of the 2023 ACM International Conference on Multimedia Retrieval*. 678–679.
- [11] Bohan Hou, Haoqiang Lin, Xuemeng Song, Haokun Wen, Meng Liu, Yupeng Hu, and Xiangyu Zhao. 2025. FIRE: Enhancing MLLMs with fine-grained context learning for complex image retrieval. In *Proceedings of the 48th International ACM SIGIR Conference on Research and Development in Information Retrieval (SIGIR)*. 803–812.
- [12] Weijian Jian, Yajun Zhang, Dawei Liang, Chunyu Xie, Yixiao He, Dawei Leng, and Yuhui Yin. 2025. Rzenembed: Towards comprehensive multimodal retrieval. *arXiv preprint arXiv:2510.27350* (2025).
- [13] Dongzhi Jiang, Renrui Zhang, Ziyu Guo, Yanmin Wu, Jiayi Lei, Pengshuo Qiu, Pan Lu, Zehui Chen, Chaoyou Fu, Guanglu Song, Peng Gao, Yu Liu, Chunyuan Li, and Hongsheng Li. 2024. MMSearch: Benchmarking the Potential of Large Models as Multi-modal Search Engines. *arXiv:2409.12959 [cs.CV]* <https://arxiv.org/abs/2409.12959>
- [14] Ziyang Jiang, Rui Meng, Xinyi Yang, Semih Yavuz, Yingbo Zhou, and Wenhui Chen. 2024. Vlm2vec: Training vision-language models for massive multimodal embedding tasks. *arXiv preprint arXiv:2410.05160* (2024).
- [15] Shyamgopal Karthik, Karsten Roth, Massimiliano Mancini, and Zeynep Akata. 2024. Vision-by-Language for Training-Free Compositional Image Retrieval. *International Conference on Learning Representations (ICLR)* (2024).
- [16] Polina Kirichenko, Mark Ibrahim, Kamalika Chaudhuri, and Samuel J Bell. 2025. AbstentionBench: Reasoning LLMs Fail on Unanswerable Questions. *arXiv preprint arXiv:2506.09038* (2025).
- [17] Mingxin Li, Yanzhao Zhang, Dingkun Long, Keqin Chen, Sibao Song, Shuai Bai, Zhibo Yang, Pengjun Xie, An Yang, Dayiheng Liu, et al. 2026. Qwen3-VL-Embedding and Qwen3-VL-Reranker: A Unified Framework for State-of-the-Art Multimodal Retrieval and Ranking. *arXiv preprint arXiv:2601.04720* (2026).
- [18] Qian Liang, Yujia Wu, Kuncheng Li, Jiwei Wei, Shiyuan He, Jinyu Guo, and Ning Xie. 2025. MM-R1: Unleashing the Power of Unified Multimodal Large Language Models for Personalized Image Generation. *arXiv:2508.11433 [cs.CV]* <https://arxiv.org/abs/2508.11433>
- [19] Tsung-Yi Lin, Michael Maire, Serge Belongie, James Hays, Pietro Perona, Deva Ramanan, Piotr Dollár, and C Lawrence Zitnick. 2014. Microsoft coco: Common objects in context. In *European conference on computer vision*. Springer, 740–755.
- [20] Fuxiao Liu, Yinghan Wang, Tianlu Wang, and Vicente Ordonez. 2021. Visual news: Benchmark and challenges in news image captioning. In *Proceedings of the 2021 conference on empirical methods in natural language processing*. 6761–6771.
- [21] Weiwen Liu, Xu Huang, Xingshan Zeng, xinlong hao, Shuai Yu, Dexun Li, Shuai Wang, Weinan Gan, Zhengying Liu, Yuanqing Yu, Zezhong WANG, Yuxian Wang, Wu Ning, Yutai Hou, Bin Wang, Chuhan Wu, Wang Xinzhi, Yong Liu, Yasheng Wang, Duyu Tang, Dandan Tu, Lifeng Shang, Xin Jiang, Ruiming Tang, Defu Lian, Qun Liu, and Enhong Chen. 2025. ToolACE: Winning the Points of LLM Function Calling. In *The Thirteenth International Conference on Learning Representations*. <https://openreview.net/forum?id=8EB8k6dDCU>
- [22] Zheyuan Liu, Cristian Rodriguez-Opazo, Damien Teney, and Stephen Gould. 2021. Image Retrieval on Real-Life Images With Pre-Trained Vision-and-Language Models. In *Proceedings of the IEEE/CVF International Conference on Computer Vision (ICCV)*. 2125–2134.
- [23] Dongchen Lu, Yuyao Sun, Zilu Zhang, Leping Huang, Jianliang Zeng, Mao Shu, and Huo Cao. 2025. Internvl-x: Advancing and accelerating internvl series with efficient visual token compression. *arXiv preprint arXiv:2503.21307* (2025).
- [24] Xueguang Ma, Sheng-Chieh Lin, Minghan Li, Wenhui Chen, and Jimmy Lin. 2024. Unifying multimodal retrieval via document screenshot embedding. *arXiv preprint arXiv:2406.11251* (2024).
- [25] Rui Meng, Ziyang Jiang, Ye Liu, Mingyi Su, Xinyi Yang, Yuepeng Fu, Can Qin, Zeyuan Chen, Ran Xu, Caiming Xiong, et al. 2025. Vlm2vec-v2: Advancing multimodal embedding for videos, images, and visual documents. *arXiv preprint arXiv:2507.04590* (2025).
- [26] OpenAI, Aaron Hurst, Adam Lerer, Adam P. Goucher, Adam Perelman, Aditya Ramesh, Aidan Clark, AJ Ostrow, Akila Welihinda, Alan Hayes, Alec Radford, Aleksander Madry, Alex Baker-Whitcomb, Alex Beutel, Alex Borzunov, Alex Carney, Alex Chow, Alex Kirillov, Alex Nichol, Alex Paino, Alex Renzin, Alex Tachard Passos, Alexander Kirillov, Alexi Christakis, Alexis Conneau, Ali Kamali, Allan Jabri, Allison Moyer, Allison Tam, Amaduo Crookes, Amin Tootoochian, Amin Tootoochian, Ananya Kumar, Andrea Vallone, Andrej Karpathy, Andrew Branstetter, Andrew Cann, Andrew Codisoti, Andrew Galu, Andrew Kondrich, Andrew Tulloch, Andrey Mishchenko, Angela Baek, Angela Jiang, Antoine Pelisse, Antonia Woodford, Anuj Gosalia, Arka Dhar, Ashley Pantuliano, Avi Nayak, Avital Oliver, Barret Zoph, Behrooz Ghorbani, Ben Leimberger, Ben Rossen, Ben Sokolowsky, Ben Wang, Benjamin Zweig, Beth Hoover, Blake Sanic, Bob McGrew, Bobby Spero, Bogo Gertler, Bowen Cheng, Brad Lightcap, Brandon Walkin, Brendan Quinn, Brian Guarraci, Brian Hsu, Bright Kellogg, Brydon Eastman, Camillo Lugaresi, Carroll Wainwright, Cary Bassin, Cary Hudson, Casey Chu, Chad Nelson, Chak Li, Chan Jun Shern, Channing Conger, Charlotte Barette, Chelsea Voss, Chen Ding, Cheng Lu, Chong Zhang, Chris Beaumont, Chris Hallacy, Chris Koch, Christian Gibson, Christina Kim, Christine Choi, Christine McLeavey, Christopher Hesse, Claudia Fischer, Clemens Winter, Coley Czarnecki, Colin Jarvis, Colin Wei, Constantin Koumouzelis, Dane Sherburn, Daniel Kappler, Daniel Levin, Daniel Levy, David Carr, David Farhi, David Mely, David Robinson, David Sasaki, Denny Jin, Dev Valladares, Dimitris Tsipras, Doug Li, Duc Phong Nguyen, Duncan Findlay, Edede Oiwoh, Edmund Wong, Ehsan Asdar, Elizabeth Proehl, Elizabeth Yang, Eric Antonow, Eric Kramer, Eric Peterson, Eric Sigler, Eric Wallace, Eugene Brevdo, Evan Mays, Farzad Khorasani, Felipe Petroski Such, Filippo Raso, Francis Zhang, Fred von Lohmann, Freddie Sulit, Gabriel Goh, Gene Oden, Geoff Salmon, Giulio Starace, Greg Brockman, Hadi Salman, Haiming Bao, Haitang Hu, Hannah Wong, Haoyu Wang, Heather Schmidt, Heather Whitney, Heewoo Jun, Hendrik Kirchner, Henrique Ponde de Oliveira Pinto, Hongyu Ren, Huiwen Chang, Hyung Won Chung, Ian Kivlichen, Ian O'Connell, Ian O'Connell, Ian Osband, Ian Silber, Ian Sohl, Ibrahim Okuyucu, Ikaai Lan, Ilya Kostrikov, Ilya

- Sutskever, Ingmar Kanitscheider, Ishaan Gulrajani, Jacob Coxon, Jacob Menick, Jakub Pachocki, James Aung, James Betker, James Crooks, James Lennox, Jamie Kiros, Jan Leike, Jane Park, Jason Brown, Jason Phang, Jason Teplitz, Jason Wei, Jason Wolfe, Jay Chen, Jeff Harris, Jenia Varavva, Jessica Gan Lee, Jessica Shieh, Ji Lin, Jiahui Yu, Jiayi Weng, Jie Tang, Jieqi Yu, Joanne Jang, Joaquin Quinonero Candela, Joe Beutler, Joe Landers, Joel Parish, Johannes Heidecke, John Schulman, Jonathan Lachman, Jonathan McKay, Jonathan Uesato, Jonathan Ward, Jong Wook Kim, Joost Huizinga, Jordan Sitkin, Jos Kraaijeveld, Josh Gross, Josh Kaplan, Josh Snyder, Joshua Achiam, Joy Jiao, Joyce Lee, Juntang Zhuang, Justyn Harriman, Kai Fricke, Kai Hayashi, Karan Singhal, Katy Shi, Kavin Karthik, Kayla Wood, Kendra Rimbach, Kenny Hsu, Kenny Nguyen, Keren Gu-Lemberg, Kevin Button, Kevin Liu, Kiel Howe, Krithika Muthukumar, Kyle Luther, Lama Ahmad, Larry Kai, Lauren Itow, Lauren Workman, Leher Pathak, Leo Chen, Li Jing, Lia Guy, Liam Fedus, Liang Zhou, Lien Mamitsuka, Lilian Weng, Lindsay McCallum, Lindsey Held, Long Ouyang, Louis Fumay, Lu Zhang, Lukas Kondraciuk, Lukasz Kaiser, Luke Hewitt, Luke Metz, Lyric Doshi, Mada Afllak, Maddie Simens, Madeleine Boyd, Madeleine Thompson, Marat Dukhan, Mark Chen, Mark Gray, Mark Hudnall, Marvin Zhang, Marwan Aljubei, Mateusz Litwin, Matthew Zeng, Max Johnson, Maya Shetty, Mayank Gupta, Meghan Shah, Mehmet Yatbaz, Meng Jia Yang, Mengchao Zhong, Mia Glaese, Mianna Chen, Michael Janner, Michael Lampe, Michael Petrov, Michael Wu, Michele Wang, Michelle Fradin, Michelle Pokrass, Miguel Castro, Miguel Oom Temudo de Castro, Mikhail Pavlov, Miles Brundage, Miles Wang, Minal Khan, Mira Murati, Mo Bavarian, Molly Lin, Murat Yesildal, Nacho Soto, Natalia Gimelshein, Natalie Cone, Natalie Staudacher, Natalie Summers, Natan LaFontaine, Neil Chowdhury, Nick Ryder, Nick Stathas, Nick Turley, Nik Tezak, Niko Felix, Nithanth Kudige, Nitish Keskar, Noah Deutsch, Noel Bundick, Nora Puckett, Ofir Nachum, Ola Okelola, Oleg Boiko, Oleg Murk, Oliver Jaffe, Olivia Watkins, Olivier Godement, Owen Campbell-Moore, Patrick Chao, Paul McMillan, Pavel Belov, Peng Su, Peter Bak, Peter Bakkum, Peter Deng, Peter Dolan, Peter Hoeschele, Peter Welinder, Phil Tillet, Philip Pronin, Philippe Tillet, Prafulla Dhariwal, Qiming Yuan, Rachel Dias, Rachel Lim, Rahul Arora, Rajan Troll, Randall Lin, Rapha Gontijo Lopes, Raul Puri, Reah Miyara, Reimar Leike, Renaud Gaubert, Reza Zamani, Ricky Wang, Rob Donnelly, Rob Honsby, Rocky Smith, Rohan Sahai, Rohit Ramchandani, Romain Huet, Rory Carmichael, Rowan Zellers, Roy Chen, Ruben Chen, Ruslan Nigmatullin, Ryan Cheu, Saachi Jain, Sam Altman, Sam Schoenholz, Sam Toizer, Samuel Miserendino, Sandhini Agarwal, Sara Culver, Scott Ethersmith, Scott Gray, Sean Grove, Sean Metzger, Shamez Hermani, Shantanu Jain, Shengjia Zhao, Sherwin Wu, Shino Jomoto, Shirog Wu, Shuaiqi Xia, Sonia Phene, Spencer Papay, Srinivas Narayanan, Steve Coffey, Steve Lee, Stewart Hall, Suchir Balaji, Tal Broda, Tal Stramer, Tao Xu, Tarun Gogineni, Taya Christianson, Ted Sanders, Tejal Patwardhan, Thomas Cunningham, Thomas Degry, Thomas Dimson, Thomas Raoux, Thomas Shadwell, Tianhao Zheng, Todd Underwood, Todor Markov, Toki Sherbakov, Tom Rubin, Tom Stasi, Tomer Kaftan, Tristan Heywood, Troy Peterson, Tyce Walters, Tyna Eloundou, Valerie Qi, Veit Moeller, Winnie Monaco, Vishal Kuo, Vlad Fomenko, Wayne Chang, Weiyi Zheng, Wenda Zhou, Wesam Manassra, Will Sheu, Wojciech Zaremba, Yash Patil, Yilei Qian, Yongjik Kim, Youlong Cheng, Yu Zhang, Yuchen He, Yuchen Zhang, Yujia Jin, Yunxing Dai, and Yury Malkov. 2024. GPT-4o System Card. arXiv:2410.21276 [cs.CL] <https://arxiv.org/abs/2410.21276>
- [27] OpenAI. 2025. OpenAI o3 and o4-mini System Card. <https://cdn.openai.com/pdf/2221c875-02dc-4789-800b-e7758f3722c1/o3-and-o4-mini-system-card.pdf>
- [28] OpenSearch-AI. 2025. Ops-MM-embedding-v1-7B. <https://huggingface.co/OpenSearch-AI/Ops-MM-embedding-v1-7B>
- [29] Bryan A Plummer, Liwei Wang, Chris M Cervantes, Juan C Caicedo, Julia Hockenmaier, and Svetlana Lazebnik. 2015. Flickr30k entities: Collecting region-to-phrase correspondences for richer image-to-sentence models. In *Proceedings of the IEEE international conference on computer vision*. 2641–2649.
- [30] Alec Radford, Jong Wook Kim, Chris Hallacy, Aditya Ramesh, Gabriel Goh, Sandhini Agarwal, Girish Sastry, Amanda Askell, Pamela Mishkin, Jack Clark, et al. 2021. Learning transferable visual models from natural language supervision. In *International conference on machine learning*. PMLR, 8748–8763.
- [31] Christoph Schuhmann, Romain Beaumont, Richard Vencu, Cade Gordon, Ross Wightman, Mehdi Cherti, Theo Coombes, Aarush Katta, Clayton Mullis, Mitchell Wortsman, et al. 2022. Laion-5b: An open large-scale dataset for training next generation image-text models. *Advances in neural information processing systems* 35 (2022), 25278–25294.
- [32] Noah Shinn, Federico Cassano, Ashwin Gopinath, Karthik Narasimhan, and Shunyu Yao. 2023. Reflexion: Language agents with verbal reinforcement learning. *Advances in Neural Information Processing Systems* 36 (2023), 8634–8652.
- [33] Yuanmin Tang, Jue Zhang, Xiaoting Qin, Jing Yu, Gaopeng Gou, Gang Xiong, Qingwei Lin, Saravan Rajmohan, Dongmei Zhang, and Qi Wu. 2025. Reason-before-retrieve: One-stage reflective chain-of-thoughts for training-free zero-shot composed image retrieval. In *Proceedings of the IEEE/CVF Conference on Computer Vision and Pattern Recognition (CVPR)*. 14400–14410.
- [34] Raghuvuvar Thirukovalluru, Rui Meng, Ye Liu, Karthikeyan K, Mingyi Su, Ping Nie, Semih Yavuz, Yingbo Zhou, Wenhu Chen, and Bhuwan Dhingra. 2025. Breaking the Batch Barrier (B3) of Contrastive Learning via Smart Batch Mining. arXiv:2505.11293 [cs.CV] <https://arxiv.org/abs/2505.11293>
- [35] Raghuvuvar Thirukovalluru, Rui Meng, Ye Liu, Mingyi Su, Ping Nie, Semih Yavuz, Yingbo Zhou, Wenhu Chen, Bhuwan Dhingra, et al. 2025. Breaking the Batch Barrier (B3) of Contrastive Learning via Smart Batch Mining. *arXiv preprint arXiv:2505.11293* (2025).
- [36] Tristan Thrush, Ryan Jiang, Max Bartolo, Amanpreet Singh, Adina Williams, Douwe Kiela, and Candace Ross. 2022. Winoground: Probing vision and language models for visio-linguistic compositionality. In *Proceedings of the IEEE/CVF Conference on Computer Vision and Pattern Recognition*. 5238–5248.
- [37] Michael Tschannen, Alexey Gritsenko, Xiao Wang, Muhammad Ferjad Naeem, Ibrahim Alabdulmohsin, Nikhil Parthasarathy, Talfan Evans, Lucas Beyer, Ye Xia, Basil Mustafa, et al. 2025. Siglip 2: Multilingual vision-language encoders with improved semantic understanding, localization, and dense features. *arXiv preprint arXiv:2502.14786* (2025).
- [38] Rong-Cheng Tu, Wenhao Sun, Hanzhe You, Yingjie Wang, Jiaying Huang, Li Shen, and Dacheng Tao. 2025. Multimodal Reasoning Agent for Zero-Shot Composed Image Retrieval. *arXiv preprint arXiv:2505.19952* (2025).
- [39] Edward Vendrow, Omiros Pantazis, Alexander Shepard, Gabriel Brostow, Kate E Jones, Oisín Mac Aodha, Sara Beery, and Grant Van Horn. 2024. INQUIRE: A natural world text-to-image retrieval benchmark. *Advances in Neural Information Processing Systems* 37 (2024), 126500–126514.
- [40] Liang Wang, Nan Yang, Xiaolong Huang, Linjun Yang, Rangan Majumder, and Furu Wei. 2024. Multilingual e5 text embeddings: A technical report. *arXiv preprint arXiv:2402.05672* (2024).
- [41] Hui Wu, Yupeng Gao, Xiaoxiao Guo, Ziad Al-Halah, Steven Rennie, Kristen Grauman, and Rogerio Feris. 2021. The Fashion IQ Dataset: Retrieving Images by Combining Side Information and Relative Natural Language Feedback. *CVPR* (2021).
- [42] Jinming Wu, Zihao Deng, Wei Li, Yiding Liu, Bo You, Bo Li, Zejun Ma, and Ziwei Liu. 2025. MMSearch-R1: Incentivizing LLMs to Search. arXiv:2506.20670 [cs.CV] <https://arxiv.org/abs/2506.20670>
- [43] Youze Xue, Dian Li, and Gang Liu. 2025. Improve Multi-Modal Embedding Learning via Explicit Hard Negative Gradient Amplifying. arXiv:2506.02020 [cs.CV] <https://arxiv.org/abs/2506.02020>
- [44] An Yang, Anfeig Li, Baosong Yang, Beichen Zhang, Binyuan Hui, Bo Zheng, Bowen Yu, Chang Gao, Chengen Huang, Chenxu Lv, et al. 2025. Qwen3 technical report. *arXiv preprint arXiv:2505.09388* (2025).
- [45] Zhongyu Yang, Wei Pang, and Yingfang Yuan. 2026. XR: Cross-Modal Agents for Composed Image Retrieval. *arXiv preprint arXiv:2601.14245* (2026).
- [46] Zhenyu Yang, Dizhan Xue, Shengsheng Qian, Weiming Dong, and Changsheng Xu. 2024. LDRE: LLM-based Divergent Reasoning and Ensemble for Zero-Shot Composed Image Retrieval. In *Proceedings of the 47th International ACM SIGIR Conference on Research and Development in Information Retrieval (SIGIR)*. 80–90.
- [47] Shunyu Yao, Jeffrey Zhao, Dian Yu, Nan Du, Izhak Shafran, Karthik R Narasimhan, and Yuan Cao. 2022. React: Synergizing reasoning and acting in language models. In *The eleventh international conference on learning representations*.
- [48] Xiaohua Zhai, Basil Mustafa, Alexander Kolesnikov, and Lucas Beyer. 2023. Sigmoid loss for language image pre-training. In *Proceedings of the IEEE/CVF International Conference on Computer Vision*. 11975–11986.
- [49] Yanzhao Zhang, Mingxin Li, Dingkun Long, Xin Zhang, Huan Lin, Baosong Yang, Pengjun Xie, An Yang, Dayiheng Liu, Junyang Lin, Fei Huang, and Jingren Zhou. 2025. Qwen3 Embedding: Advancing Text Embedding and Reranking Through Foundation Models. arXiv:2506.05176 [cs.CL] <https://arxiv.org/abs/2506.05176>

A Details of Dataset Construction

Here we provide the complete prompts and detailed methods for each stage of the PHOTOBENCH construction pipeline. All prompts are designed both in Chinese and in English. Here we only show the English version

A.1 Event Narrative Update Prompt

Incremental Event Narrative Synthesis

Role: Precise Event Analyst. **Objective:** Iteratively refine a coherent narrative from clustered images.

Logic Protocol:

- **Initial (Index 0):** Establish baseline hypothesis from visual cues.
- **Update (Intermediate):** Synthesize new details or advance storyline using temporal connectors (e.g., “then”, “afterward”). Correct earlier assumptions if contradictions arise.
- **Final (Index $N - 1$):** Produce a polished, globally consistent summary.

Constraints: Continuous narrative (no lists); Evidence-based inference (e.g., cake \rightarrow birthday); Eliminate redundancy; Retroactively refine for causal coherence.

A.2 Intention Inference Prompt

Context-Aware Capture Intention Inference

Objective: Infer the primary motivation behind a photo by synthesizing behavioral trajectory and visual content.

Analysis Framework:

- (1) **Trajectory Mapping:** Analyze the user’s preceding activity sequence.
- (2) **Role Identification:** Define the photo’s functional role (milestone, routine, or climax) within the event chain.
- (3) **Motivation Mapping:** Categorize intent (e.g., memory preservation, information retrieval, artistic expression, or social sharing).

Output: A single declarative sentence (e.g., “Recording a specific exhibit detail for future reference”). No meta-talk or labels.

A.3 Query Generation Prompt

Intent-Driven Multimodal Query Generation

Task: Generate 3 diverse, colloquial queries reflecting the user’s search psychological state.

Generation Dimensions:

- **Event-centric:** Focus on the macro-activity (e.g., “beach camping”).
- **Object-centric:** Focus on key subjects and states (e.g., “cat sun-bathing”).
- **Freeform:** Focus on atmosphere, color, or specific metadata constraints.

Requirements: Incorporate person nicknames; Use metadata naturally; Keep queries < 15 characters; Omit filler words like “photo of”.

Output Format: JSON with queries and reasoning (mapping intent to query logic).

A.4 Zero-GT queries Synthesis Method

We generate zero-GT queries in two ways:

- **Metadata Perturbation and Semantic Variation:** We employ metadata perturbation by introducing contradictions such as conflicting timestamps, and modify key relational roles (e.g., changing family roles) to create plausible but non-existent descriptions. For semantic variation, we alter key elements in the query, such as modifying relationships or context, making the description realistic but still without a corresponding match in the dataset.
- **Query Variations:** We also create variations on existing queries by three methods: (1) Entity Mismatch: Replace the subject in a query with a rare or unrelated entity (e.g., changing *birthday party with Alice* to *birthday party with a celebrity*). (2) Scene Mismatch: Place individuals in unusual or unexpected settings, such as an unlikely career or an unfamiliar outdoor scene (e.g., *changing meeting at a restaurant with colleagues* to *meeting in a foreign office*). (3) Detail Enhancement: Add specific or uncommon details to a query, such as including rare actions or unique props, making the matching process significantly more difficult.

These zero-GT queries undergo the same verification process described in Section 3.2.3, where human experts confirm that no relevant ground-truth images exist in the dataset for these queries.

A.5 Zero-GT Query Generation Prompt

Zero-Ground Truth (Zero-GT) Synthesis

Goal: Synthesize “unfulfillable” queries that are contextually plausible but lack visual matches to test system rejection capabilities.

Methodology:

- **M1: Semantic Deviation:** Shift entities or scenes to realistic but absent variants; hyper-specify details to make matches statistically impossible.
- **M2: Constraint Injection:** Append conflicting metadata to valid queries (e.g., a year the user never visited that location, or a location where the specific activity never occurred).

Constraints: Maintain realism (no sci-fi); Colloquial style; Verified via exhaustive VL-model cross-check to ensure zero matches.

B Implementation Details of Metrics

B.1 Metrics for Query Linguistic Analysis

To facilitate the reproduction of our linguistic analysis of queries, we provide the formal definitions and algorithmic implementations for the metrics presented in Figure 3. All metrics are computed using the `en_core_web_sm` model from the `spaCy` NLP library.

B.1.1 Average Query Length and Noun Density. The **Average Query Length** is defined as the mean number of tokens per query. **Noun Density** (ρ_n) measures the concentration of informational entities within a query, calculated as the ratio of nouns and proper nouns to the total token count:

$$\rho_n = \frac{\sum_{i \in T} \mathbb{I}(\text{pos}(i) \in \{\text{NOUN}, \text{PROPN}\})}{|T|}$$

where T is the set of tokens in a query, and $\mathbb{I}(\cdot)$ is the indicator function.

B.1.2 Average Syntactic Depth. **Syntactic Depth** quantifies the structural complexity of a query. For each input, we generate a

dependency parse tree. The depth of a tree D is the maximum path length from the root node to any leaf node:

$$D = \max_{n \in \text{nodes}} (\text{path_length}(\text{root}, n))$$

For multi-sentence queries, we record the maximum depth across all constituent sentences. A lower depth indicates a flatter, more fragmented grammatical structure typical of search-style interactions.

B.1.3 Lexical Diversity (MTLD). We adopt the **Measure of Textual Lexical Diversity (MTLD)** to evaluate vocabulary richness. Unlike the simple Type-Token Ratio (TTR), MTLD is robust against variations in total corpus length.

The calculation follows a sequential factor-based approach:

- (1) **Factorization:** The algorithm traverses the token sequence until the TTR drops below a predefined threshold (set to 0.72 in our implementation). At this point, a “factor” is completed, and the TTR calculation resets.
- (2) **Bidirectional Scoring:** This process is performed both forward (F_{fwd}) and backward (F_{bwd}) through the corpus to ensure stability.
- (3) **Final Calculation:** The MTLD score is the ratio of the total number of tokens N to the average number of factors:

$$\text{MTLD} = \frac{N}{(F_{fwd} + F_{bwd})/2}$$

A higher MTLD score signifies that the dataset utilizes a broader and more specialized vocabulary.

B.2 Metrics for System Rejection Ability Evaluation

To evaluate the rejection capability of a system, we regard an *empty prediction* as a rejection event. Given a test set $\{(g_i, p_i)\}_{i=1}^N$, let $\mathbb{I}(\cdot)$ be the indicator function and define

$$E(x) = \mathbb{I}(x = \emptyset).$$

We compute the following counts:

$$A = \sum_{i=1}^N \mathbb{I}(E(g_i) = 1 \wedge E(p_i) = 1), \quad B = \sum_{i=1}^N \mathbb{I}(E(g_i) = 0 \wedge E(p_i) = 1),$$

$$C = \sum_{i=1}^N \mathbb{I}(E(g_i) = 1 \wedge E(p_i) = 0), \quad D = \sum_{i=1}^N \mathbb{I}(E(g_i) = 0 \wedge E(p_i) = 0),$$

where A is correct rejection, B is false rejection, C is missed rejection, and D is correct non-rejection.

Reject-Precision, Reject-Recall, and Reject-F1 are defined as:

$$\text{Reject-Precision} = \frac{A}{A+B}, \quad \text{Reject-Recall} = \frac{A}{A+C},$$

$$\text{Reject-F1} = \frac{2 \cdot \text{Reject-Precision} \cdot \text{Reject-Recall}}{\text{Reject-Precision} + \text{Reject-Recall}} = \frac{2A}{2A+B+C}.$$

Reject-Precision measures the *correctness* of rejection decisions (*i.e.*, how often rejected cases truly have empty ground truth), Reject-Recall measures the *coverage* of rejection (*i.e.*, how many empty-ground-truth cases are successfully rejected), and Reject-F1 provides a single summary by *balancing* Reject-Precision and Reject-Recall, penalizing both over-rejection (B) and under-rejection (C).

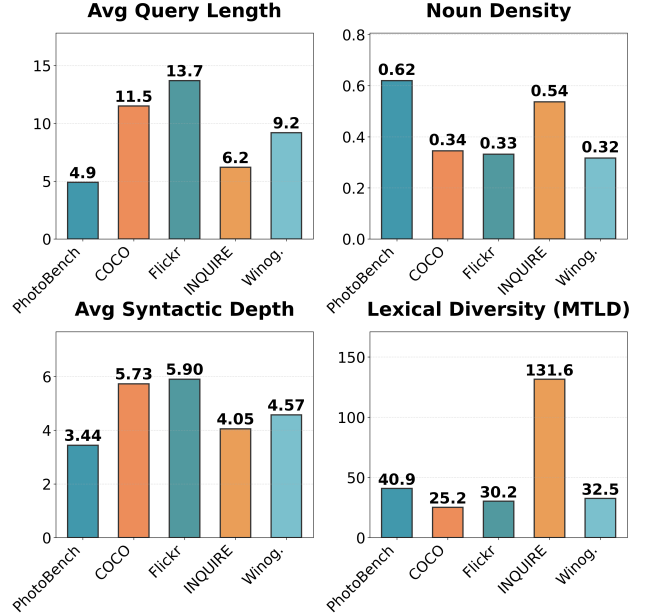


Figure 3: Linguistic comparison with traditional benchmarks. We evaluate four dimensions: Avg Query Length (total tokens), Noun Density (proportion of entities), Avg Syntactic Depth (grammatical complexity), and Lexical Diversity (MTLD, measuring vocabulary richness independent of text length). PhotoBench queries are structurally streamlined (lower length and depth) yet lexically diverse, reflecting search-style rather than narrative-style language.

C Extended Dataset Statistics

C.1 Comparison with classic benchmarks

As shown in Figure 3, PHOTOBENCH exhibits a linguistic profile distinct from traditional narrative benchmarks. To quantify the transition from “descriptive narration” to “search-style” retrieval, we evaluate queries across two dimensions: structural complexity (Length and Syntactic Depth) and semantic concentration (Noun Density and MTLD).

Unlike the verbose, clause-heavy captions in COCO2014 and Flickr30k, our queries are characterized by structural conciseness—favoring short, noun-phrase-centric inputs with significantly lower syntactic depth. This efficiency-first approach reflects how users prioritize intent over grammatical ornamentation. Crucially, this brevity does not equate to semantic simplicity; PHOTOBENCH consistently outperforms standard benchmarks in Lexical Diversity (MTLD), indicating a more specialized and diverse vocabulary tailored to personalized contexts. Technical formulations for these metrics are detailed in Appendix B.1

C.2 Per-Album Statistics

Table 7 provides detailed statistics for each album in PHOTOBENCH. **Album Diversity.** The three albums represent distinct user archetypes:

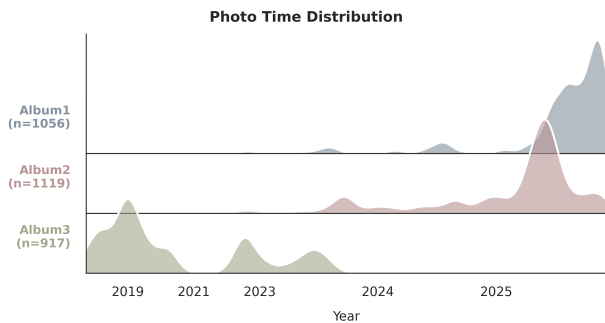
Table 7: Per-album statistics. Albums vary in social density (Core Faces) and visual patterns (Portrait ratio), ensuring benchmark diversity.

Album	# Images	Metadata (%)	Portrait (%)	Core Faces
Album 1	1,069	97.7	7.3	10
Album 2	1,466	75.7	43.5	2
Album 3	1,047	76.7	24.6	8
Total	3582	83.4	25.1	20

- **Album 1** (event-centric): High metadata coverage (97.7%), low portrait ratio (7.3%), many social connections (10 core faces). Typical of users who document activities and locations.
- **Album 2** (person-centric): Highest portrait ratio (43.5%), fewer core faces (2). Typical of users focused on family/couple documentation.
- **Album 3** (balanced): Moderate across all dimensions. Representative of general-purpose personal albums.

C.3 Temporal Distribution

Figure 4 illustrates the temporal span of our benchmark, covering a diverse period from 2018 to 2025. Notably, the peak activities across the three albums are staggered and complementary. When one album exhibits a sparsity of data, another often compensates with a high density of photos. This interleaved distribution ensures a relatively uniform aggregate density over an extensive timeline, preventing temporal bias while providing a robust testbed for evaluating a model’s long-range temporal reasoning and retrieval consistency.

**Figure 4: Temporal distribution of photos across albums.**

D Supplementary Analysis: The Fact vs. Cognitive Dimension

In this section, we introduce an exploratory taxonomy and its corresponding experiments. Despite the compelling theoretical motivation, current model bottlenecks prevent the results from fully manifesting the expected performance distinctions at this stage.

D.1 Motivation and Taxonomy

Initially, we hypothesized that the primary bottleneck in personal photo retrieval lies in the **reasoning depth** required by a query.

To investigate this, we developed a dual-layer taxonomy focusing on five semantic dimensions: *Location*, *Time*, *Person*, *Object*, and *Concept*.

As defined in Table 8, each dimension in a query is annotated as either **Fact-based** (requiring direct perceptual mapping) or **Cognitive** (requiring inferential reasoning, world knowledge, or personal context). Crucially, within a single dimension, these labels are mutually exclusive, though a single query often spans multiple dimensions (e.g., “photos with my girlfriend at home” involves Cognitive labels in both *Person* and *Location* dimensions).

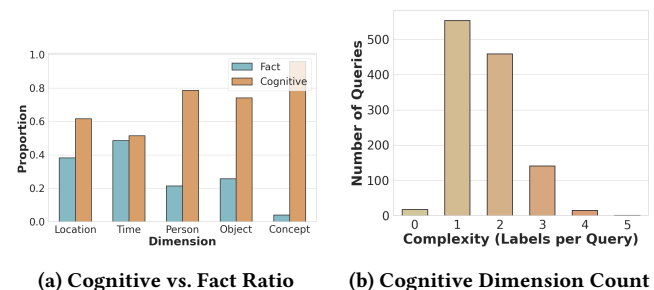
Table 8: The Dual-Layer Taxonomy across five dimensions. Fact-based queries involve explicit signal matching; Cognitive queries require reasoning synthesis.

Dimension	Fact-based (Explicit)	Cognitive (Implicit)
Location	“in Shanghai”	“at home,” “at the gym”
Time	“in May 2024”	“during Spring Festival”
Person	“Zhang Wei”	“with my girlfriend”
Object	“a red car”	“the parking spot before the concert”
Concept	“sunset”	“cozy moments with family”

D.2 Statistical Distribution

We annotated our entire dataset using this framework. Figure 5 illustrates the distribution:

- **Dimension Ratio (a)**: Shows the prevalence of Cognitive vs. Fact labels across dimensions. Cognitive requirements are most prominent in *Time* and *Concept* dimensions.
- **Cognitive Complexity (b)**: Shows the number of Cognitive labels per query. A value of “0” denotes a purely Fact-based query or one with no specific dimension tags. Most queries involve 1–2 cognitive dimensions, confirming the inferential nature of real-world photo searches.

**Figure 5: Supplementary query statistics. (a) Distribution of labels across semantic dimensions. (b) Distribution of Cognitive labels per query (0 indicates a pure Fact-based query).**

D.3 The Counterintuitive Result

Our analysis revealed a surprising trend: the “Cognitive Gap” is not the primary performance driver. As shown in Table 9, embedding models actually perform *better* on Cognitive queries than on Fact queries (−28.52 gap).

Table 9: Performance by reasoning depth (Recall@10). Embedding models show a negative gap (better on Cognitive), while agents show a slight positive gap.

Method Type	Fact	Cognitive	Gap
Best Embedding	35.24	63.76	-28.52
Best Agent	78.60	70.98	+7.62

Interpretation: Modality Gap Masks Reasoning Gap. For embedding models, the lower Fact performance is largely a byproduct of the **Modality Gap**: many Fact-based queries are Metadata-dependent (e.g., specific dates or locations), which are invisible to visual embeddings. Conversely, many Cognitive queries (e.g., “cozy moments”) possess strong visual signatures that embeddings can capture through semantic similarity, even without explicit reasoning.

For agents, Cognitive queries are slightly more challenging due to the **Source Fusion Paradox**: resolving multiple implicit dimensions requires complex tool-calling and information pruning, which increases the likelihood of error propagation.

D.4 Conclusion

While the Fact/Cognitive distinction provides an intuitive lens, our empirical data suggests that **information-source accessibility (VMF)** is a more actionable diagnostic axis. We therefore prioritize the VMF taxonomy in our main analysis.

E Additional Experiments on English Version of PHOTOBENCH

This part presents additional experiments on the English version of PHOTOBENCH. Overall, the experimental results are consistent with our primary findings. This demonstrates the generalizability of our benchmark and confirms that the observations are language-independent. Table 10 is the English version of Table 4.

Table 10: Recall@10 performance decomposition by source-aware query types (English Version).

Type	Agent(A)	Multimodal(M)	Text(T)	$\Delta(A-M)$	$\Delta(A-T)$
S_V	71.5	77.3	73.3	-5.8	-1.9
S_M	53.4	6.5	7.8	+46.9	+45.6
S_F	69.4	12.4	4.9	+57.1	+64.5
S_{VM}	62.0	65.8	63.4	-3.8	-1.3
S_{VF}	42.6	57.8	47.5	-15.1	-4.9
S_{MF}	57.0	13.0	8.3	+44.0	+48.7
S_{VMF}	39.4	54.8	43.9	-15.4	-4.5

F Experimental Protocol of Commercial System

For commercial system evaluation, we followed this standardized procedure:

- (1) Factory reset each device to ensure clean state.
- (2) Transfer all album images via USB.
- (3) Allow 24 hours for on-device indexing and automatic organization to complete.
- (4) Issue queries via native gallery search interface.
- (5) Record all returned results (up to 100 per query).
- (6) Two annotators independently verified result relevance.

G Case Study Gallery

This section presents additional case studies illustrating the contrast between embedding-based and agentic retrieval.

G.1 Case: Functional Intent

Query: “The receipt I used for reimbursement on my last business trip”

Analysis: This query requires: (1) identifying “business trip” events from trajectory logs, (2) locating the most recent occurrence, and (3) finding receipt-like images within that specific temporal window.

Embedding Result: Returns visually similar receipt images from various time periods, including unrelated personal purchases, due to a lack of temporal and logical constraints.

Agent Result: Correctly identifies the specific business trip event (e.g., 3 weeks ago), filters the search to that time range, and then isolates receipt images, successfully returning the correct documentation.

G.2 Case: Social Context

Query: “Photos of New Year’s Eve dinner with my parents”

Analysis: This requires: (1) resolving “parents” to specific face IDs via identity metadata, (2) identifying the specific Spring Festival timeframe, and (3) locating dining-related images containing those specific individuals.

Embedding Result: Returns generic dinner scenes and family photos without temporal specificity, failing to distinguish the holiday context.

Agent Result: Utilizes `identity_lookup` for parents, filters for the Lunar New Year period, and identifies dining scenes, correctly retrieving the specific celebration photos.

G.3 Case: False Memory (Zero-GT)

Query: “Sunset photos at the beach last summer”

Ground Truth: No beach photos exist in the user’s album for the specified period.

Embedding Result: Returns sunset photos from other locations and beach photos from different years—yielding false positives due to partial visual matching.

Agent Result: Executes a filtered search for beach locations within the summer timeframe, finds no matches, and correctly returns an empty result set with a logical explanation.

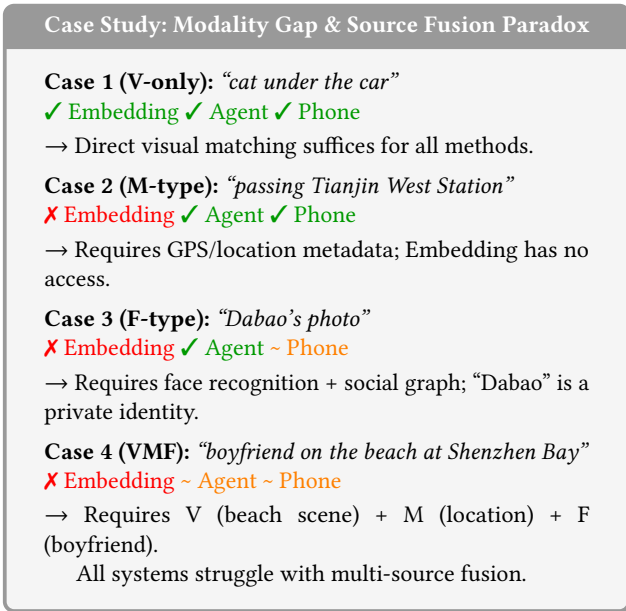


Figure 6: Case study illustrating the Modality Gap and Source Fusion Paradox. ✓=success, ~=partial, ✗=failure.

G.4 Case: Query types

Figure 6 illustrates representative query cases across different source types, as well as the performance of different methods:

Case 1 (V-only): Query: “cat under the car”. All approaches succeed—direct visual matching suffices.

Case 2 (M-type): Query: “passing Tianjin West Station”. Embedding fails completely (no location reasoning); Agent and Phone succeed via metadata filtering.

Case 3 (F-type): Query: “Dabao’s photo”. Embedding fails as it cannot resolve private identities. Agent succeeds via Face Engine; Phone performance varies by vendor.

Case 4 (VMF): Query: “boyfriend on the beach at Shenzhen Bay”. This requires visual scene understanding, location/time metadata, and face recognition simultaneously. All systems show degraded performance, demonstrating the Source Fusion Paradox.

H Agentic Retrieval Framework

While the main text evaluates a general-purpose agentic baseline for benchmarking, this section details a specialized, multi-stage Agentic Retrieval Framework specifically architected for the nuances of personal photo management, which is illustrated in Fig. 7. Compared to the standard agent, this framework introduces a more sophisticated orchestration layer to handle the semantic complexity of gallery-based queries.

As illustrated in Fig. 7, the architecture leverages a unified 4B Vision-Language Model to function as the internal Planner, Evaluator, and captioning engine, ensuring cross-task consistency. The underlying retrieval stage is powered by a high-efficiency 2B VLM-based embedding model.

The framework adopts a three-phase routing mechanism: it first executes rule-based matching, followed by intent-driven distribution to either metadata lookups or hybrid retrieval. For complex queries requiring deeper reasoning, the system escalates to the agentic planner to synthesize results. Preliminary results in Table ?? demonstrate that our framework achieves a superior F1 score of 62.07%, outperforming existing baselines. These findings suggest that optimizing agentic coordination is a promising direction for enhancing retrieval performance in on-device mobile environments.

I Agentic Retrieval Framework

While the main text evaluates a general-purpose agentic baseline for benchmarking, this section details a specialized, multi-stage Agentic Retrieval Framework (illustrated in Fig. 7) specifically architected for the nuances of personal photo management. Compared to the standard agent, this framework introduces a more sophisticated orchestration layer to handle the semantic complexity of gallery-based queries.

The architecture leverages a unified 4B Vision-Language Model (VLM) to function as the Planner, Evaluator, and captioning engine, while the underlying retrieval stage is powered by a 2B VLM-based embedding model. Orchestrating these components is a three-phase routing mechanism that initiates with rule-based matching, progresses to intent-driven distribution—directing queries to either metadata lookups or hybrid retrieval—and ultimately escalates complex requests requiring deeper reasoning to the agentic planner for comprehensive result synthesis.

As shown in Table 11, our framework achieves the best overall performance, with the highest F1 score of 63.3% on normal queries and the strongest rejection capability (Rej-F1 of 52.0%). While our recall (70.2%) is slightly lower than the best agentic baseline, this is primarily due to our significantly smaller retrieval model (2B parameters) compared to large-scale models. These findings suggest that optimizing agentic coordination with lightweight on-device models is a promising direction for enhancing retrieval performance in mobile environments.

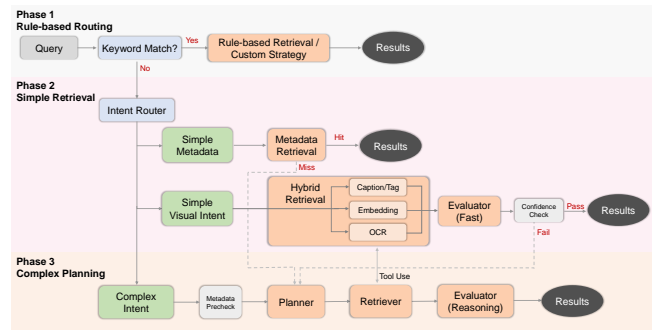


Figure 7: The proposed hierarchical agentic framework architecture for photo retrieval.

Table 11: Performance of our proposed agentic framework on PHOTOBENCH. All values in %. “P”, “R”, “Rej-P”, “Rej-R” and “Rej-F1” denote Precision, Recall, F1, Reject-Precision, Reject-Recall and Reject-F1, respectively.

System	Normal Query			Zero-GT Query		
	P	R	F1	Rej-P	Rej-R	Rej-F1
Ours	67.3	70.2	63.3	50.8	53.3	52.0
ToolACE-2	38.3	54.7	39.0	15.1	<u>35.0</u>	21.1
Qwen3-8B	37.6	68.1	41.0	16.8	16.7	16.7
Qwen3-32B	39.6	66.3	41.4	16.7	25.8	20.3
DeepSeek-v3	38.5	66.2	40.7	11.8	10.0	10.8
Qwen3-235B-A22B	<u>50.8</u>	71.6	<u>51.9</u>	14.3	6.7	9.1
GPT-4o	45.4	65.3	46.4	13.8	17.5	15.4
OpenAI-o3	44.6	<u>75.2</u>	48.0	<u>34.5</u>	33.3	<u>33.9</u>
Claude-Sonnet-4.5	43.7	78.3	47.9	14.3	8.3	10.5
Claude-Opus-4.5	46.9	74.7	50.5	18.2	13.3	15.4

J Statement on Evaluation Discrepancies

Current commercial mobile retrieval systems are often highly optimized for specific visual perception scenarios (e.g., identity documents, visual objects, or pets) using specialized models and hard-coded metadata rules. We clarify that our benchmark is not intended to provide an exhaustive evaluation of every fine-grained visual category. Furthermore, due to the difference in evaluation dimensions and data distributions, it is both expected and reasonable that our results may diverge from phone manufacturers’ internal benchmarks. Our primary objective is to evaluate the system’s capability to holistically satisfy complex and deep-seated retrieval intents, moving beyond simple recognition to deep semantic understanding.